Turun yliopisto
University of Turku

SPECTRALLY TUNED LANTHANIDE PHOTOLUMINESCENCE FOR POINT-OF-CARE TESTING

Timo Valta

TURUN YLIOPISTON JULKAISUJA – ANNALES UNIVERSITATIS TURKUENSIS
Sarja - ser. AI osa - tom. 520 | Astronomica - Chemica - Physica - Mathematica | Turku 2015

University of Turku

Faculty of Mathematics and Natural Sciences
Department of Biochemistry
Molecular Biotechnology and Diagnostics
Doctoral Programme in Molecular Life Sciences

Supervised by

Carina Horn, PhD
Diabetes Care
Roche Diagnostics GmbH
Mannheim, Germany

Professor Tero Soukka, PhD
Department of Biochemistry
Molecular Biotechnology and Diagnostics
University of Turku
Turku, Finland

Reviewed by

Adjunct Professor Harri Hakala, PhD
Perkin Elmer, Wallac
Turku, Finland

Thomas Hirsch, PhD
Institute of analytical chemistry
Chemo- and biosensors
University of Regensburg
Regensburg, Germany

Opponent

Professor Ingo Klimant, PhD
Institute of Analytical Chemistry and
Food Chemistry
Graz University of Technology
Graz, Austria

The originality of this thesis has been checked in accordance with the University of Turku quality assurance system using the Turnitin OriginalityCheck service.

ISBN 978-951-29-6187-0 (PRINT)
ISBN 978-951-29-6188-7 (PDF)
ISSN 0082-7002
Painosalama Oy - Turku, Finland 2015

"Life is too short to write long things."

— Stanisław J. Lec

CONTENTS

LIST OF ORIGINAL PUBLICATIONS

This thesis is based on the following publications, referred to in the text by their Roman numerals (I-IV).

I Valta, T., Puputti, E-M., Hyppänen, I., Kankare, J., Takalo, H. & Soukka, T. Ligand enabling visible wavelength excitation of europium(III) for fluoroimmunoassays in aqueous micellar solutions. Anal. Chem. **84**, 7708–7712 (2012).

II Horn, C. & Valta, T. Composition comprising up-converting phosphors for detecting an analyte. WO/2015/078899 [Patent application].

III Valta, T., Kale, V., Soukka, T. & Horn, C. Near-infrared excited ultraviolet emitting upconverting phosphors as an internal light source in dry chemistry test strips for glucose sensing. Analyst **140**, 2638–2643 (2015).

IV Valta, T. & Horn, C. Upconverting phosphors as an amplifier of a colorimetric signal in dry chemistry test strips for enzymatic measurement of glucose. [Accepted manuscript]

In addition, unpublished data are included.

ABBREVIATIONS

β-NTA	2-naphthoyltrifluoroacetone
βHCG	The β-subunit of hCG gonadotropin
ASSURED	Affordable, sensitive, specific, user-friendly, rapid and robust, equipment-free, delivered
bdc	A ligand for Eu(III) with the structure of 9-ethyl-3,6-bis(5′,5′,5′,4′,4′-pentafluoro-1′,3′-dioxopentyl)carbazole
bio-BSA	Biotinylated bovine serum albumin
CCD	Charge-coupled device
CKMB	Creatine kinase MB
cNAD	Carba-nicotinamide adenine dinucleotide
CRP	C-reactive protein
CT	Charge transfer
CV	Coefficient of variation
DELFIA	Dissociation-enhanced lanthanide fluorescent immunoassay
DES	DELFIA enhancement solution
ELISA	Enzyme-linked immunosorbent assay
ESA	Excited-state absorption
ETU	Energy transfer upconversion
Eu-SA	Europium labelled streptavidin
HPV	Human papillomavirus
ILCT	Intraligand charge transfer
IR	Infrared
LED	Light-emitting diode
LF	Lateral flow
LMCT	Ligand-to-metal charge transfer
MLCT	Metal-to-ligand charge transfer
NAD^+	Oxidized form of nicotinamide adenine dinucleotide
NADH	Reduced form of nicotinamide adenine dinucleotide
NIR	Near-infrared
NT-proBNP	N-terminal of the prohormone brain natriuretic peptide
PMo	Phosphomolybdenum blue
PMT	Photomultiplier tube
POC	Point-of-care
S/N	Signal-to-noise
SA	Streptavidin
TOPO	Trioctylphosphine oxide

UCμP	Upconverting microphosphor
UCNP	Upconverting nanophopshor
UCP	Upconverting phosphor
UV	Ultraviolet
VIS	Visible
WHO	World health organization

ABSTRACT

Point-of-care (POC) –diagnostics is a field with rapidly growing market share. As these applications become more widely used, there is an increasing pressure to improve their performance to match the one of a central laboratory tests. Lanthanide luminescence has been widely utilized in diagnostics because of the numerous advantages gained by the utilization of time-resolved or anti-Stokes detection. So far the use of lanthanide labels in POC has been scarce due to limitations set by the instrumentation required for their detection and the shortcomings, e.g. low brightness, of these labels. Along with the advances in the research of lanthanide luminescence, and in the field of semiconductors, these materials are becoming a feasible alternative for the signal generation also in the future POC assays.

The aim of this thesis was to explore ways of utilizing time-resolved detection or anti-Stokes detection in POC applications. The long-lived fluorescence for the time-resolved measurement can be produced with lanthanide chelates. The ultraviolet (UV) excitation required by these chelates is cumbersome to produce with POC compatible fluorescence readers. In this thesis the use of a novel light-harvesting ligand was studied. This molecule can be used to excite Eu(III)-ions at wavelengths extending up to visible part of the spectrum. An enhancement solution based on this ligand showed a good performance in a proof-of-concept -bioaffinity assay and produced a bright signal upon 365 nm excitation thanks to the high molar absorptivity of the chelate. These features are crucial when developing miniaturized readers for the time-resolved detection of fluorescence.

Upconverting phosphors (UCPs) were studied as an internal light source in glucose-sensing dry chemistry test strips and ways of utilizing their various emission wavelengths and near-infrared excitation were explored. The use of nanosized $NaYF_4$:Yb^{3+},Tm^{3+}-particles enabled the replacement of an external UV-light source with a NIR-laser and gave an additional degree of freedom in the optical setup of the detector instrument. The new method enabled a blood glucose measurement with results comparable to a current standard method of measuring reflectance. Microsized visible emitting UCPs were used in a similar manner, but with a broad absorbing indicator compound filtering the excitation and emission wavelengths of the UCP. This approach resulted in a novel way of benefitting from the non-linear relationship between the excitation power and emission intensity of the UCPs, and enabled the amplification of the signal response from the indicator dye.

TIIVISTELMÄ

Vieritestaus on nopeasti laajeneva diagnostiikan osa-alue. Näiden sovellusten yleistyminen asettaa myös vaatimuksia niiden suorituskyvylle, jonka tulisi ideaalitapauksessa yltää keskuslaboratoriotestien tasolle. Lantanidien luminesenssia on jo pitkään hyödynnetty diagnostisissa sovelluksissa johtuen niiden lukuisista eduista, joita saavutetaan käytettäessä aikaerotteista tai käänteisviritykseen perustuvaa mittaustekniikkaa. Tähän asti lantanidileimojen käyttö vieritestauksessa on kuitenkin ollut vähäistä, johtuen niiden havainnointiin käytettyjen laitteistojen ja itse leimojen rajoituksista. Näissä tapahtuneen kehityksen myötä lantanidileimat ovat jo varteenotettava vaihtoehto entistä parempien vieritestien kehitykseen.

Tämän väitöstyön tavoitteena oli tutkia tapoja hyödyntää aikaerotteista ja käänteisviritysmittaustapaa vieritestauksessa. Aikaerotteisen mittauksen vaatima pitkäikäinen fluoresenssi voidaan tuottaa lantanidikelaateilla, joiden viritys tapahtuu perinteisesti ultraviolettiaallonpituuksilla. Tämän virityksen tuotto on kuitenkin hankalaa vieritestaukseen soveltuvalla mittalaitteella. Tässä väitöstyössä tutkittiin uuden ligandin käyttöä Eu(III)-ionin virityksessä. Tutkitun ligandin viritysspektri ylsi näkyvän valon aallonpituuksille ja soveltui käytettäväksi bioaffiniteettimäärityksessä. Uusi kehitysliuos toimi hyvin mallina käytetyssä bioaffiniteettimäärityksessä ja tuotti voimakkaan signaalin 365 nm virityksellä johtuen kelaatin suuresta molaarisesta absorptiviteetista. Nämä ominaisuudet ovat keskeisiä, kun kehitetään vieritestaukseen soveltuvia, pienikokoisia mittalaitteita aikaerotteisen fluoresenssin mittaukseen.

Käänteisviritteisiä partikkeleita puolestaan käytettiin sisäisinä valonlähteinä veren glukoosipitoisuutta mittaavissa testiliuskoissa, hyödyntäen näiden partikkelien lähi-infrapunaviritystä ja lukuisia emissioaallonpituuksia. Nanokokoisten $NaYF_4$:Yb^{3+},Tm^{3+}-partikkeleiden käyttö mahdollisti ulkoisen ultraviolettivalonlähteen korvaamisen lähi-infrapunalaserilla ja mittalaitteen optisen kokoonpanon vapaamman suunnittelun. Uusi mittaustapa tuotti tuloksiltaan standardimenetelmään verrattavan suorituskyvyn. Mikrokokoisia, näkyvän valon aallonpituuksilla emittoivia käänteisviritteisiä partikkeleita hyödynnettiin vastaavalla tavalla, mutta käyttäen laajalla aallonpituusalueella absorboivaa indikaattoriyhdistettä, suodattaen sekä partikkelien emissio- että viritysaallonpituuksia. Tämä menetelmä mahdollisti uuden tavan hyödyntää näiden partikkelien viritys- ja emissiotehon välistä epälineaarista suhdetta ja mahdollisti indikaattoriyhdisteen tuottaman signaalin vahvistamisen.

1 INTRODUCTION

Point-of-care (POC) testing is an area of diagnostics that refers to a test performed near the patient or the treatment facility. This provides rapidly crucial information related to the treatment without the need to send the sample to a central laboratory. Various forms of POC testing are already used regularly, including measurement of blood glucose, pregnancy tests, and detection of markers for acute coronary syndrome. POC assays have been shown to have several benefits including reduced frequency of hospital visits, travel expenses, and lost work time.[1] They can also improve clinical decision making, patient satisfaction, and adherence to prescribed medication.[2,3] Patients using POC tests are also more careful with their lifestyle[4] and take a more active part in their treatment[5]. However, some applications require higher sensitivity[6] or a lower limit of detection than can be attained by the current methods[7].

Lanthanide chelates[8] and upconverting phosphors[9] have proven themselves as valuable luminescent label technology in various diagnostic applications. These labels have already shown a tremendous potential in some POC-applications as they can be used to improve the detection limit of the assays by utilizing time-resolved[10,11] or anti-Stokes detection[12,13]. Despite the promising results, the use of lanthanide labels in POC has been scarce so far, partially due to the lack of proper instrumentation[10,11,14–16]. However recent advances in light-emitting diodes (LEDs)[17], detectors[18], and photoluminescent lanthanide materials[19,20] are now removing these obstacles.

In this thesis, new ways of utilizing lanthanide labels in POC-assays have been studied by investigating the use of a new type of enhancement solution for Eu(III)-ions, that could potentially be used with a miniaturized reader. Upconverting phosphors have been studied as an internal light source in glucose sensing test strips. The following literary review will focus on providing an overview on the current POC technologies, their shortcomings, and on how lanthanide labels could be used to overcome them. The feasibility of utilizing lanthanide labels in POC assays is also discussed.

2 REVIEW OF THE LITERATURE

2.1 Point-of-care –testing

2.1.1 History

The history of point-of-care testing can be said to trace a long way back into the history (1500 BCE), when it was discovered that ants were drawn to the urine of certain people. This may well have been the earliest method to diagnose glucose in the urine, a sign of diabetes. In the medieval times this technique was refined by having a physician taste the urine and look for the sweet taste of glucose. The English physician Thomas Willis first reported this method in 1674, describing the taste of diabetic urine as "wonderfully sweet as if it were imbued with honey or sugar". Luckily for the physicians, chemical testing made the tasting unnecessary in the 20th century. The first tests were performed by heating urine with Benedict's reagent, when the glucose in the urine would reduce the copper-ions in the solution and turn the colour from blue to red.[21]

Further improvement came with the launch of Clinistix in 1956[22]. These test strips utilized enzymes for a more specific reaction and there was no longer need to heat the urine. The results could be observed as a colour change on the test strips, but the results remained semi-quantitative at best. Urine remained as the sample material for long as it is easily accessible and easy to deal with. Despite these benefits, measuring glucose in urine is a rather insensitive and nonspecific method that only shows the elevation in blood glucose while hypoglycemia remains undetected. To account for these issues, the first test strips for detecting glucose in blood were developed already in 1964[23]. Just like with test strips for urine, the method of detection was to observe the formation of colour on the strip and to compare this to a reference chart to estimate the amount of glucose in the blood. In order to improve the interpretation of the results, an instrument was introduced in 1969 to measure reflectance from the test strips[24]. Despite the testing getting rather easy to perform, most of it was still done in a hospital setting by professionals and the idea of letting the patients perform the tests themselves at home was a rather controversial issue[21] until 1975[25]. This was soon followed by the introduction of the first home pregnancy test in 1976[26].

Self-monitoring of blood glucose was among the very first point-of-care test, and nowadays perhaps the most widely used one in the world with numerous other tests also available and new ones constantly under development. According to the BCC

Research LLC[27], the rapidly growing POC market is expected to reach 19.3 billion US dollars by the year 2018 as a result of a rising number of lifestyle diseases and a trend towards healthcare decentralization.

2.1.2 Benefits of POC-testing

Despite the higher cost-per-test compared to a central laboratory testing, POC-assays can bring tremendous benefits to various areas of healthcare. In-home testing has been shown to reduce frequency of hospital visits, travel expenses, and lost work time[1]. POC-testing can also improve clinical decision making, patient satisfaction, and adherence to prescribed medication.[2,3] Patients using POC tests are also more careful with their lifestyle (e.g. diet and alcohol consumption) and have a higher degree of compliance because they are more motivated[4] and take a more active part in the treatment[5].

In order to evaluate POC tests, the world health organization (WHO) has listed a set of requirements that an ideal POC test should fulfill.[28] These requirements are known by the acronym ASSURED, standing for: affordable, sensitive, specific, user-friendly, rapid and robust, equipment-free, delivered.[29]

2.1.3 POC-technologies

It should be noted that point-of-care is a very broad term and its definition has undergone some changes over the years, one of the latest being "a diagnostic test that is performed near the patient or treatment facility, has a fast turnaround time, and may lead to a change in patient management"[30]. The actual circumstances, where the testing is performed, may range from a modern hospital environment in a high-income country with electricity and trained personnel available, to a rural area in a low-income country lacking electricity and trained personnel[31]. As also each analyte and sample matrix present their own requirements, there is no one-size-fits-all -solution and different POC application can be divided into a wide spectra of technologies as done by Luppa et al[32]. They have divided the POC analysers into six categories based on their sensor characteristics, complexity, measuring mode, underlying detection principle and sample matrix. According to this classification, the POC tests span from rather simple lateral flow assays all the way to tremendously sophisticated lab-on-a-chip -type of solutions. The result may be a simple qualitative colour formation, interpretable with the naked eye, or a quantitative signal, requiring a dedicated reader.

Depending on the assay, the actual platform for a POC test can be e.g. a disposable strip, chip or a cartridge, that contains the necessary reagents, and possibly also fluidics, optics, electrodes etc. The sample matrix is preferably something easily obtainable, such as saliva or urine, but often also blood or other bodily fluid containing the analyte. One of the main challenges of the POC devices is the small sample volume usually something from hundreds of nanoliters to around a milliliter with analyte concentrations from femto- to millimolar.[33]

2.1.4 Signal generation techniques

Current methods

Optical techniques are usually considered as the "gold standard" as the signal generation technique in POC assays[34–36] and they are applied to several tests already on the market[33]. In comparison to the other market leader, electrochemical detection, optical methods may have a lower cost per test[37], a greater aptitude for miniaturization[31] and a better multiplexing capability[37].

As mentioned before, the interpretation of a result from a POC test may be a mere visual inspection of a line formed by e.g. gold nanoparticles[38] on a home pregnancy test, or comparing the intensity of a formed colour to a reference picture as in early glucose test strips. This is without a doubt the simplest method as it requires no instrumentation for the detection[33], but is not sensitive and precise enough for most of the applications. With a simple instrumentation to detect the absorbance or reflectance, it is possible to improve the interpretation compared to visual detection [39,40]. However, the small dimensions (e.g. on a microchip) pose severe problems for a sensitive and reliable absorbance measurement[7]. As the sample volume decreases, the optical path length through the sample decreases and this affects the measurement as described by the Beer-Lambert law. Several signal amplification strategies have been developed in order to overcome this issue utilizing noble metals[41,42] nanoparticles, and enzymes[41] with excellent results. However these methods generally require additional liquid handling steps increasing the time and work required. For assays such as lateral flow, label which give direct signal are preferable.[43]

An example of a case where the current methods are starting to fall short are the blood glucose meters. They are generally based on detecting the enzymatic reaction with glucose either photometrically (by the change of colour) or amperometrically (by the electric current produced by the reaction). Many of these meters struggle to meet the limit of accuracy required[6,44] and Rebel *et al*[6] simply state that "Development of a

meter with accuracy equal to central laboratory devices should continue to be the industry goal".

Ways of improving assay sensitivity

Several different optical technologies can be used in POC tests to improve their performance. These include, among others, fluorescence, chemiluminescence, surface plasmon resonance and light scattering.[33] Each of these techniques has their advantages and drawbacks, and selecting the optimal one is often down to the specific application. Especially in the case of POC, it comes down to balancing cost, sensitivity, complexity, reproducibility, portability and power requirements.[34]

Fluorescence is generally considered as the most popular technique requiring only a rather simple instrumentation producing a highly specific signal with detection limits down to 10^{-9}-10^{-13} mol/L.[36] It is the most widely used optical method for microsensing systems[33] due to its superior selectivity, sensitivity and many colours available[45,46]. The conventional fluorophores still fall short of the label required for an ideal microfluidic device, defined by Gervais *et al*[35], enabling the detection of analytes down to the concentration range of 10^{-12}-10^{-15} mol/L. Many fluorophores also have issues such as high autofluorescence background, photobleaching, short luminescence lifetime, and/or toxicity. They also suffer from self-quenching, when the local fluorophore concentration is too high, e.g. when the labelling degree of a tracer molecule is too high.

The single most prominent drawback affecting the assay sensitivity is the presence of an unspecific signal originating either from excitation light leaking to the detection window, or from autofluorescence. Autofluorescence originates from various sources including the sample vessel as well as the sample itself. A typical biological sample, e.g. serum, contains several fluorescent substances such as nicotinamide adenine dinucleotide (NAD^+/H)[47], and several plastics may pose issues for excitation wavelengths of up to 550 nm[48]. Due to autofluorescence, the detection limits of various labels are 50- to 1000-fold lower in a serum than in a buffer.[49] Proper sample pretreatment can be used to minimize these problems, but it can be cumbersome[50] and ideally also difficult matrices, such as whole blood, could be used for assays[51]. Several strategies have been employed to minimize the issue of autofluorescence, including the use of confocal optics[52], two-photon excitation[53], fluorescent labels with excitation and emission in the near-infrared (NIR) part of the spectrum[54] or large Stokes shift[55], modulating the analyte migration velocity and employing lock-in detection[48], as well as optimizing the vessel material[56].

Common features for these interferences are that they have a short or no lifetime (autofluorescence and leaked excitation light) and occur at higher wavelengths compared to the excitation. Lanthanide based labels have proven themselves interesting alternatives for the common fluorescent labels[57,58] as they offer a convenient way to circumvent these issues with time-resolved or anti-Stokes detection.

2.2 Lanthanide photoluminescence

Lanthanides are a group of 14 elements with atomic numbers from 57 to 71 (from lanthanum to lutetium). These elements are extensively used in many modern applications including the production of renewable energy, electronics, and lighting. They are commonly also referred to as the rare earth elements, a name that stems from the misconception that these elements are extremely scarce. There is however a large variation in their rarity and some of the lanthanides are actually more abundant in the earth's crust than all of the precious metals[59]. What makes lanthanides rare, is that they are rarely concentrated into ore deposits like most commercially mined metals[60].

Due to several applications, the global demand of lanthanides is expected to exceed 160 000 tons in 2015, measured in rare earth oxides[60]. As the demand increases there is also an interest towards new mining processes with the environmental aspects taken into consideration[61], as several cases of lanthanide mining have been associated with contamination of the local environment[62]. The value of luminescent lanthanide materials may be considered through the fact that, according to some estimations, in 2012 luminescent materials account for one third of the commercial value of the annually extracted lanthanides, while representing less than 10 percent of their tonnage.[19]

The remarkable properties of lanthanides originate from their electronic structure. They usually exist as trivalent cations giving them the electronic configuration of $[Xe]4f^n$, where *n* represents the number of electrons in the 4f shells and varies from 0 to 14 when moving through the lanthanide series from La(III) to Lu(III). The 4f orbitals are shielded by the 5s and 5p subshells[63], which is the key to the chemical and spectroscopic properties of these ions. The chemical properties of lanthanides differ only slightly from each other due to their decrease in size along with the increasing atomic number[64], making the separation of lanthanides challenging and costly[65].

What makes one lanthanide different from another, is their optical properties. Apart from lanthanum and lutetium, lanthanides have the ability to produce

photoluminescence in various wavelengths that cover the spectrum from ultraviolet (UV) to NIR[66]. These emissions originate from the transitions between the shielded 4f orbitals, which results in sharp bands with exceptionally long lifetimes[67]. The majority of the lanthanides have been employed as photoluminescent labels in diagnostics in one way or another, but a handful of these have received most of the attention. The diagnostic applications of these ions are divided into time-resolved fluorometry (utilizing mainly europium, terbium, dysprosium, and samarium) and upconversion (erbium, holmium, thulium, and ytterbium).

The electronic transitions that take place between the 4f orbitals are so called Laporte-forbidden transitions.[67] This has two implications in terms of fluorescence. As the transitions are forbidden (or rather, have a low probability of occurring), the molar absorptivities of lanthanide ions are extremely low ($< 10\ M^{-1}cm^{-1}$)[68]. Because of this, the direct excitation of lanthanides is an extremely unlikely event. However when the ion gets to an excited state, it may stay there up to millisecond timescale as also the relaxation is a forbidden process. The issue of excitation can be overtaken by placing the ion into an organic or inorganic environment containing excitation absorbers acting as antennas or sensitizers for the ion. The absorbed energy can then be transferred to the lanthanide ion. Placing the lanthanide ion in a ligand-field also disturbs its symmetry, partially relaxing the Laporte selection rule, making the transitions partially allowed.[67]

The emission wavelength of the lanthanide is determined by the energy difference between the excited and ground state. The location of the states is determined by various forces affecting the electrons in the 4f-orbitals. As these electrons have very little interaction with the chemical environment of the ion, the energy states are determined by the interactions within the ion. The different states of the free ion are described by the Russell-Saunders[69] term symbol $^{2S+1}L_J$, where $2S+1$ represents the total spin multiplicity giving the number of possible electron spin orientations, L the total orbital angular momentum and J the total angular momentum of the f electrons. The repulsion between the electrons within the f-orbitals has the most impact on the energy level of each state designated by the term ^{2S+1}L. These states are further split into J-levels by the spin-orbit coupling. The splitting caused by the ligand-field is one order of magnitude smaller than the effect of the spin-orbit coupling and appears merely as a fine structure of the individual band, often ignored.[64]

2.3 Lanthanide chelates

2.3.1 Adjusting the excitation wavelength of Eu(III) chelates

The classical excitation pathway

The excitation of Eu(III) using an organic ligand as a light harvesting complex was originally reported by Weissman already in 1942[70]. The use of europium as a label in immunoassays was suggested by Wieder[71] and then by Soini and Hemmilä[49]. The first application of the DELFIA (dissociation-enhanced lanthanide fluoroimmunoassay), the most successful lanthanide-based immunoassay system reported to date, was finally published in 1983[72]. Since then several lanthanide ions have been used in bioanalytical applications[73], but Eu(III) is by far the most common[58].

The most common energy transfer pathway for the excitation of lanthanides with organic ligands is through the triplet pathway (^{1}S -> ^{3}T -> Ln) (Figure 1). In this pathway the ligand is first excited to the singlet state (^{1}S), originating from the aromatic transitions (π -> π^* or n -> π^*) of unsaturated structures of the ligand with a high molar absorptivity (10^4-10^5 $M^{-1}*cm^{-1}$)[74,75]. The energy is then transferred through an intersystem crossing to the triplet state (^{3}T) of the ligand from where the energy transfer to the lanthanide ion happens.[67] In the case of e.g. DELFIA system, the excitation wavelengths needed is 320-340 nm.

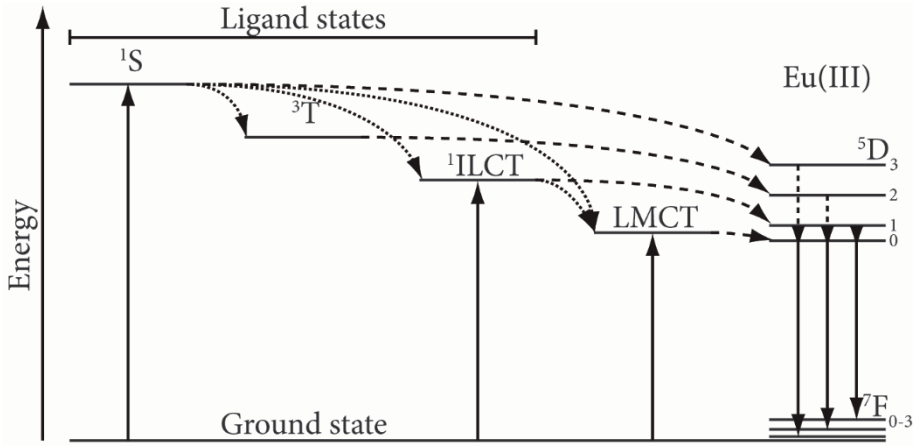

Figure 1. Schematic representation of energy absorption (upward solid arrows), migration between energy states (dotted arrows), transfer to lanthanide (dashed arrows) and emission (downward solid arrows) processes in a lanthanide complex. ^{1}S = singlet state, ^{3}T= triplet state, ^{1}ILCT = singlet intraligand charge transfer state, LMCT = ligand-to-metal charge transfer state. Ligand fluorescence, phosphorescence, and non-radiative relaxations have been omitted for the sake of clarity. Adapted from[76,77].

Excitation in the UV-range, however, has certain downsides to it. Many materials are not transparent in the UV-range and thus cannot necessarily be used with these labels. The UV absorption may also lead to high levels of autofluorescence, and damage especially biological sample material. Also a pulsed UV-excitation, suitable for the excitation of fluorescent labels, can be rather cumbersome to produce. This is usually done with a xenon flash lamp operating at a high voltage. These lamps produce an extremely wide range of wavelengths, extending from the far UV to IR, which is excessive for the purpose of fluorescence excitation, as only a small fraction of the light, produced by the lamp, is utilized and the rest will have to be filtered out. Nitrogen lasers are an alternative excitation source, but they are expensive, suffer from low repetition rate and have to be shielded as they produce electromagnetic interference.[78] Some excitation sources and detectors may also require additional choppers[79].

Light emitting diodes (LEDs) offer an interesting alternative as an excitation source. As they are small, cheap, and produce a rather narrow emission with a low voltage, they would enable the construction of significantly simpler and cheaper fluorescence readers. Unfortunately, LEDs that are powerful enough to be used as an excitation source, are available at wavelengths starting from 365 nm.[80] In order to use LEDs as an

excitation source several new ligands have been developed that enable the excitation of europium at longer wavelengths. These will be presented in the following paragraphs.

The theoretical maximum excitation wavelength for the triplet pathway is estimated by Steemers *et al*[81] to be 385 nm due to the certain energy differences required between the different states to prevent back transfer of the excitation energy.[81] Generally, the excitation wavelength can be shifted longer by expanding the π-conjugated system of the antenna ligand. Even though the location of the singlet state is of main interest when tuning the excitation wavelength of a lanthanide chelate, equally important in the triplet pathway is the location of the triplet state as it has a tremendous impact on the quantum yield of the complex[82–84]. Utilizing the triplet pathway, chelates that have excitation extending far beyond the theoretical maximum of 385 nm, to 400 nm[85,86] and even up to 500 nm[87–89] have been reported. These compounds are generally fluorinated β-diketonates with a highly conjugated aromatic moiety.

Energy transfer directly from the singlet state to the lanthanide (^{1}S -> Ln) has also been studied intensively[90–93], however the efficiency of this pathway is low because of the competing processes such as ligand fluorescence, non-radiative relaxation, and intersystem crossing[94].

Excitation through charge transfer states

In addition to the triplet state, various other states of the ligand and the lanthanide may take part in the energy transfer process (Figure 1). These include two different charge transfer (CT) states, namely intraligand CT state (ILCT) and ligand-to-metal CT state (LMCT). These states can either work as pathways when energy, absorbed via singlet state, is transferred to the lanthanide, or they can work as energy absorbers.

ILCT is an electron transfer process that occurs within the ligand. The ILCT state generally has high absorptivity with excitation wavelengths up to 485 nm. This pathway produces also higher quantum yields compared to several other excitation pathways utilized for europium chelate complexes.[66,95,96] However, the sensitization of Eu(III) through ILCT was not recognized until 2004[93] and many of the previous studies may be falsely interpreted as merely an exceptionally small singlet-triplet gap[97]. Since then several studies regarding the role of ILCT in the excitation of Eu(III) have been published[95,98–103]. In order to obtain the charge transfer, these ligands often have a strong electron donating group, such as an amino moiety connected by a conjugated structure to the lanthanide binding part of the ligand[102].

The LMCT state can be considered as a hybrid state from the mixing of ligand and lanthanide orbitals[94]. As the LMCT state tends to overlap with other states, it can be difficult to detect[104]. For example, a chelate with dpt-ligand (2-(N,N-diethylanilin-4-yl)-4,6-bis(3,5-dimethylpyrazol-1-yl)-1,3,5-triazine)) was reported to display a direct energy transfer from the ligand singlet state to the lanthanide[93]. Later it has been reported, that a LMCT state may also be involved in this process[94]. The LMCT state is essential when sensitizing lanthanides in inorganic compounds[19], however, in lanthanide chelates it is more commonly known as a source for quenching[90,105–108]. LMCT can play a role in the migration of energy from the ligand singlet state to the lanthanide[76,94] and direct absorption of LMCT has also been demonstrated, though the absorptivity was rather low[101,105].

Using d-metal complexes as antennas

A rather new approach is to use d-metal complexes as energy absorbers by utilizing the metal-to-ligand charge transfer (MLCT). These ligands have moieties for binding the lanthanide, and the d-metal ion on the same complex. The energy is absorbed by the singlet charge-transfer state of the d-metal ligand complex (^{1}MLCT) and transferred to the lanthanide via triplet state (^{3}MLCT). These complexes have several advantages over the traditional ligands such as low energy triplet states, relatively high intersystem crossing quantum yield from the singlet to triplet state and a rather long triplet excited state lifetime improving the energy transfer to the lanthanide.[66,109,110] Several d-metals have been utilized in the sensitization of lanthanides including Ru[111–113], Os[114] and Re[115–118]. However, only Ir[119–121] and Pt[122,123] have energy states suitable for the excitation of Eu(III) at wavelengths extending up to 500 nm[110].

Generally it can be noted, that the ligand triplet states (either ^{3}T or ^{3}MLCT) are the preferable donor states, when transferring the excitation energy to the lanthanide ion. As these states have longer excited state lifetime than singlet states (e.g. ^{1}S or ^{1}ILCT), the energy transfer is more likely to occur.[19]

Suitability for aqueous solutions

The majority of the studies regarding the energy transfer processes in lanthanide chelates are carried out in organic solvents as water is an efficient quencher of lanthanide luminescence. However, as practically all diagnostic assays are performed in an aqueous solution, the lanthanide chelates should be functional also in the presence of water.

Despite the difficulties presented by water, chelates with excitation extending up to 400-450 nm have been reported[97,124–127]. Due to the quenching effect of water[128], quantum yields of these complexes vary between 1 and 20 %, which is significantly lower than the highest reported value of 79 %[89] measured in solid state. In comparison, the DELFIA Enhancement Solution has an overall quantum yield of 70 %[129] and many organic fluorophores reach even higher numbers (e.g. fluorescein 85 %[130]).

2.3.2 Lanthanide chelate containing particles

Thanks to the elimination of autofluorescence, lanthanide chelates usually provide excellent sensitivity in bioaffinity assays despite their low brightness compared to many other fluorophores. However, when constructing miniaturized readers, the power of the excitation source (e.g. LEDs) and the sensitivity of the detector (e.g. photodiodes) are generally lower than in larger tabletop readers. Therefore, the brightness of an individual chelate may not be high enough to be efficiently detected and the signal of an individual label has to be increased.

Packing lanthanide chelates in nanoparticles produces labels with high brightness as one particle can accommodate thousands of chelates. Because of the wide Stokes shift of the chelate, they are not self-quenched despite the high local concentration.[131] The particle also protects the chelates from interaction with the environment[132], including the quenching effect from water[133] and some serum components[134]. This can be a valuable feature in homogenous assays where no washing steps are performed. The use of particles has produced excellent results also with chelates excitable at the visible wavelengths. Several monodispersed particles with excitation at the visible range have been reported[135–139] with quantum yields of 31 % and excitation up to 475 nm[139].

2.3.3 Applications of time-resolved fluorometry in diagnostics

General principle

The long lifetime of lanthanide fluorescence can be utilized in diagnostics to eliminate the nonspecific background signal originating from autofluorescence with time-resolved detection, provided that the lifetime of the lanthanide emission is at least 10 times longer than the one of the background signal[49]. In practice the measurement is performed with a pulsed excitation followed by a delay, during which the autofluorescence (from various sources e.g. plastic and organic material) has time to drop down to a negligible level, before the signal collection is started (Figure 2). Practically all of the emission detected in this time-window originates from the

lanthanide label providing excellent detection limits, which broadens the linear range of the assays due to the low background signals.[58]

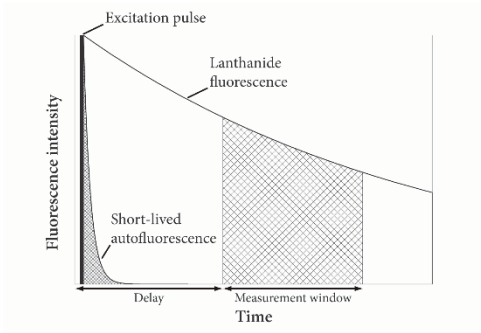

Figure 2. The principle of the time-resolved fluorescence measurement.

The first utilization of europium ions in bioaffinity assay was based on the use of an enhancement solution for heterogeneous assays, commercialized under the name of DELFIA by Wallac Oy. In this technique the lanthanide ion is bound to the detector molecule with a carrier ligand, that forms a non-luminescent complex with the lanthanide ion. When the bioaffinity reaction is completed, the ion is released from the carrier ligand and bound by the antenna ligand in a micellar chelating environment. This technique has been later refined to work also in the presence of disturbing agents[140] and the PerkinElmer Citations Library[141] reveals well over 300 publications related to DELFIA.

Due to the release of the lanthanide ion, this technique can't be utilized in applications where the signal has to be localized (e.g. imaging and flow cytometry), or where the signal has to be obtained before the reaction endpoint (e.g. real-time PCR). Therefore, a large number of intrinsically fluorescent chelates have been developed to address this issue[142–147]. They enable the use of lanthanide fluorescence in several assay technologies such as simpler heterogeneous assays[148], real-time PCR[149], various homogeneous bioaffinity assays[150,151], and lanthanide-based probes[152].

POC application

Few commercial applications related to the use of lanthanide chelates in point-of-care –diagnostics have been introduced so far. These are the AQT90 FLEX – immunoanalyzer[153,154] from Radiometer Medical ApS and GenomEra-system[155–158] from Abacus Diagnostics Oy. Both of these platforms are based on an automated tabletop analyzer that analyses the sample with minimal pretreatment. Several tests are

available including cardiac troponin I and T, creatine kinase MB (CKMB), myoglobin, NT-proBNP (N-terminal of the prohormone brain natriuretic peptide), CRP (c-reactive protein), βhCG (human chorionic gonadotropin) and D-dimer from whole blood and plasma for the AQT90 FLEX and methicillin-resistant *S. aureus*, *C. difficile*, *Streptococcus B* and *pneumoniae* from various sample materials for the GenomEra.

One of the most common point-of-care –technologies are the lateral flow assays, and the use of nanoparticles embedded with Eu(III)-chelates as a label with this technology has been widely studied and assays for eosinophiles and neutrophiles[15], C-reactive protein[159], prostate spesific antigen[10], and *P. stewartii*[11] have been published. Generally nanoparticles with Eu(III) are highly suitable for lateral flow assays and improvements on the assay sensitivities, in comparison to gold nanoparticles, have been reported[10,11]. Juntunen *et al*[10] also concluded that, due to the large Stokes shift of Eu(III)-chelates, a good assay performance was achieved even with only pulsed detection and continuous detection.

Several publications have been underlining the benefits of Eu(III)-chelates[160,161] and -nanoparticles[162,163] in POC immunoassays, and presented new technologies to be used with them, such as the chelate complementation[164]. Eu(III)-chelate embedded nanoparticles have been utilized on microchip immunoassays to produce high enough signal without the need for enzymatic signal amplification[14]. Some examples from the limits of detection obtained with europium labels can be found from e.g. the work of Pettersson *et al*[160]. They present an assay for C-reactive protein using Eu(III)-chelates as a label, with a limit of detection of 0.01 mg/L. Hyytiä *et al*[165] on the other hand have reported an assay for cardiac troponin I utilizing Eu(III)-nanoparticles with an impressive limit of detection of 0.41 ng/L. However, a significant drawback in the utilization of lanthanide chelates and nanoparticles in POC devices, is the lack of a compact reader[10,11,14,15].

2.3.4 Instrumentation used for the detection of Eu(III)-chelates

It is already possible to benefit from lanthanide chelates with a tabletop analyser as they can accommodate the traditional bulky components needed for the time-resolved detection of lanthanides, and they are plugged to an electric outlet that satisfies the power requirements of these components. For assays, such as lateral flow, a hand-held reader is often a crucial requirement and it is not feasible to fit the commonly used components (xenon flash lamp and photomultiplier tube), in a battery-operated, portable device.

Excitation of Eu(III)-chelates with LEDs has been reported on few occasions, such as on a temperature sensor based on Eu(III)-chelate in a polymer film[166,167]. The chelates in question had excitation spectra extending up to 425 nm and a quantum yield of 40 % (under 405 nm excitation in toluene at 25 °C). The chelates were efficiently excited with LEDs up to 450 nm[167] (the output power of the LEDs was not reported). LED-excitation of Eu(III)-chelates has also been studied in flow cytometry[168] and time-resolved microscopy[169–171]. In flow cytometry a 100 mW LED emitting at 365 nm was used to detect *Giardia lamblia* cysts with Eu(III)-chelate as a label. The chelate in question had an excitation maximum at 340 nm, extending up to 380 nm (the quantum yield was not reported)[172]. Similar Eu(III)-chelates and nanoparticles[169–171] were used for imaging, utilizing also a 365 nm LED as an excitation source, that proved to be a potential option for a traditional flash lamp[171]. However, all of these studies have used a photomultiplier tube or a bulky CCD-camera (charge-coupled device) as a detector, which means they are by no means small and portable.

Many groups have also attempted to construct their own miniaturized readers to detect Eu(III)-nanoparticles on lateral flow test strips[11,15,159], but this area of research seems to be shrouded in mystery as, despite the claims of excellent results, details are usually not reported. Photodiodes are generally considered as light detectors for miniaturized fluorescence readers. Rundström *et al*[15] report to have used the combination of 385 nm LED and photodiode with Eu(III)-nanoparticles on lateral flow strips, with a detection limit of $3.3*10^7$ particles/mm^2. The particles in question had a diameter of 120 nm and an excitation maximum around 340 nm[131]. No further details regarding the instrument are mentioned. Song and Knotts[159] have reported that a 365 nm LED was not powerful enough for their application using commercial Eu(III)-particles. Unfortunately, they have not revealed further details about the LED or the label. Zhang *et al*[11] claim to have developed a compact and sensitive reader. However, no details about the reader have been reported.

Despite the many drawbacks of the photomultiplier tubes (cost, high voltage, lack of robustness), they are still the most sensitive detector available despite the advances made with photodiodes. Recently a device called micro photomultiplier tube has been introduced by the company Hamamatsu Photonics. This device is marketed as one to have the sensitivity of a PMT but being extremely small and also suitable for portable POC-applications. However, as this component has just been introduced, no publications regarding its performance have yet been published.

2.4 Upconverting phosphors

2.4.1 Theory of upconversion and upconverting materials

General background

Upconversion (also known as anti-Stokes photoluminescence) is a mechanism where the energies of two or more low energy excitation photons (generally near-infrared) are combined to produce one emission photon with higher energy. This is made possible by the ladder-like distribution of long-lived energy levels of certain lanthanide ions. With modern upconverting materials it is possible to produce various emissions ranging from UV- to NIR-range with a 980 nm excitation.[173] Upconverting phosphors (UCPs) are inorganic particles consisting of a lattice, doped with the emitter ion (activator). Usually also sensitizer ions are used in conjunction with the activators.

It is also possible to produce anti-Stokes fluorescence through multiphoton absorption[174] or triplet-triplet annihilation[175]. However, the multiphoton absorption requires a high power (10^6-10^9 W/cm^2) pulsed excitation source, whereas relatively low power (1-10^3 W/cm^2)[176] is enough for the UCPs. This can be easily produced with a low cost laser diode.[177] The triplet-triplet annihilation requires low excitation power (~10 W/cm^2)[175] and has attracted much attention to be used in solar cells[178], but so far no diagnostic applications have been reported.

Theoretically, most lanthanide ions can produce upconversion when embedded in an inorganic lattice[173], but the most efficient activators are Er(III) and Tm(III)[179]. These two ions produce also a wide variety of emissions, and it is possible to cover most of the spectrum from UV to NIR wavelengths with them (Figure 3). Ho(III) can be occasionally encountered in some applications. It has an emission spectrum relatively similar to Er(III), but a lower efficiency so it is not as widely used.

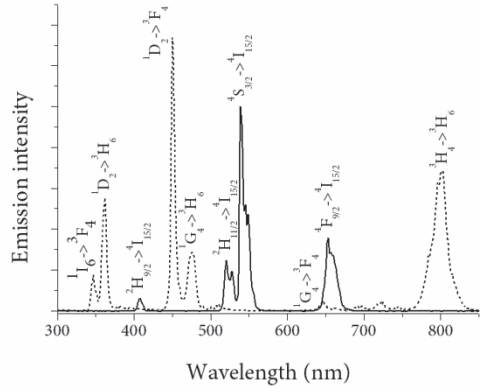

Figure 3. The anti-Stokes emissions of Er(III) (solid line) and Tm(III) (dashed line) under 980 nm excitation cover a wide range of wavelengths. The spectra are adapted from Vuojola *et al*[180] ($NaYF_4$:Yb^{3+},Er^{3+}) and Kale *et al*[181] ($NaYbF_4$:Tm^{3+}).

The sensitizer ion is used to harvest the excitation energy and to transfer it non-radiatively to the activator. This can be considered analogous to the use of an antenna ligand in lanthanide chelates as discussed in the previous chapter. Ytterbium is a common sensitizer ion as it conveniently has only one excited state, which matches well with the different energy levels of the activators. For a lanthanide, ytterbium has a relatively large absorption cross-section of $11.7*10^{-21}$ cm^2 that is about an order of magnitude larger than that of erbium[182]. However, this is still between four and five orders of magnitude lower than the antenna ligands used with lanthanide chelates. Therefore, ytterbium is commonly used in relatively large concentrations and the doping content is usually around 20 mol-%[176]. Some studies have gone a lot further and dopant levels up to 98 mol-% have been reported[183].

Optical processes leading to upconversion

The use of an activator is more or less an assumption when producing efficiently upconverting particles. This enables the production of upconversion through a process called the energy transfer upconversion (ETU) (Figure 4). It is possible to produce upconversion also without the sensitizer ion through a process called the excited-state absorption (ESA).[176] This process refers to a sequential absorption of two excitation photons by a single activator ion. Even though the long lived excited states of the lanthanide ions make this possible, the excitation power required is still too high for many practical applications and it is less efficient than the ETU by about two orders of magnitude.[184]

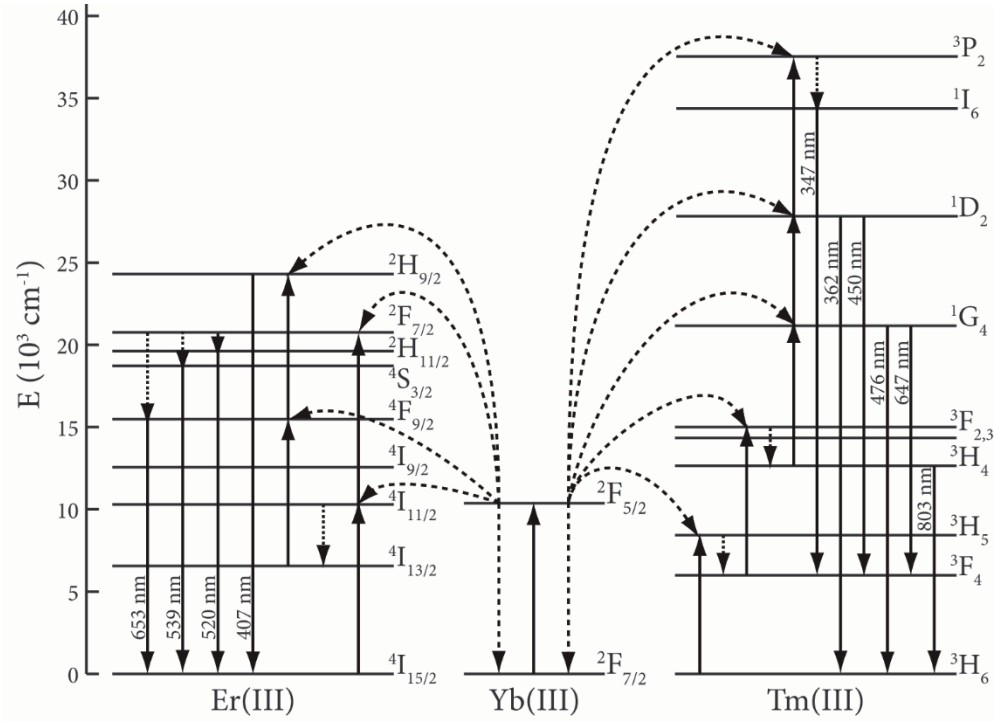

Figure 4. Proposed energy transfer mechanisms in Yb(III)-Er(III) and Yb(III)-Tm(III) pairs, under 980 nm excitation. Solid upward arrows represent excitation, dashed arrows energy transfer processes, dotted arrows relaxations and solid downward arrows emissions. Adapted from Dong *et al*[176]. and Sun *et al*[185].

Excitation and emission wavelengths of UCPs

When a sensitizer ion is used to absorb the excitation, it mainly determines the excitation wavelength of the UCP. In the case of ytterbium, this is roughly 980 nm. However, this is not the optimal wavelength to all of the applications since water has a relatively high absorption in that region and can cause heating when a high intensity excitation is applied[186]. Therefore the use of Nd(III) as an additional sensitizer together with Yb(III) has also been studied[186–189]. As Nd(III) can be excited at 808 nm, absorption of water is 24 times lower than at 980 nm[186].

The locations of the emission peaks of UCPs are determined by the activator ion, but the ratios of the different emissions and the overall luminescence quantum yield of the particle depend on various parameters. The lattice, while optically inert, plays a crucial role in determining the upconversion efficiency. Several materials have been studied for this[9], but so far β-$NaYF_4$ is considered the best host material to produce

upconversion[190,191]. In addition to this, the particle size, and ion doping concentrations all affect the UCP emission[192].

The effect of particle size on UCP emission

A lot of effort has been put into making UCPs as small as possible, as sub-10 nm particles are preferable to bioimaging applications[193]. Such particles have been synthesized[194–196] but, as mentioned previously, particle size has a large impact on the emission properties of an upconverting phosphor. As the size of the particle decreases, the surface area to volume –ratio increases and the surface effects become critical at diameters under 20 nm[194]. Therefore a relatively higher number of surface defects and a higher ratio of the optically active ions that are exposed to the environment. Both of these can result in non-radiative transitions that quench the UCP emission[195,197]. More specific studies have shown that both the UCP quantum yield[198] and emission lifetimes[194,196,199] decrease with the particle size. Protecting the particles with a shell of undoped lattice material has commonly been used to overcome these issues[194–196,200,201]. Gargas *et al*[194] have determined that for UCPs with a diameter of 8 nm, the optimal shell thickness is about 1.8 nm. These core-shell structures have also been used in various ways to enhance the emission and to tune the optical properties of UCPs.[20,202]

Drawbacks of UCPs

There is also a good reason to study ways of enhancing the emission intensity of UCPs as the low brightness is a common drawback. The reported absolute quantum yields of $NaYF_4$:Yb^{3+},Er^{3+} particles vary between 0.0022-3.5 %[196,198] depending on the particle size (<10 nm to bulk) and dopant concentrations. It should be noted, that opposed to traditional fluorophores, the theoretical maximum quantum yield of UCPs can never be 100 %. As upconversion is a multiphoton process, a rough number would be 100 %/n, where *n* is the average number of excitation photons required to produce one emission photon. This is still not taking into account a significant portion of the excitation photons lost as down shifting emission.[203] Only few results have been reported so far as the non-linear nature of upconversion makes the measurement and comparison of these results rather complicated, as the UCP quantum yield depends also on the excitation intensity.

As the light harvesting ability of lanthanides is limited by the low absorptivity, attempts have been made to overcome this by using organic infrared dyes as antenna molecules with UCPs. This approach also broadens the excitation spectrum to the shorter wavelengths. With this approach, Zou *et al*[204] managed to increase the

integrated spectral response of the UCPs 3 300-fold. Plasmonic field enhancement has been studied in various ways[205] with upconversion enhancement up to 450-fold.

In order to conjugate infrared dyes or binder molecules on the UCP, proper functional groups will first have to be introduced on the particle surface. This modification step is required also to render the particles dispersable in aqueous solution, as the particles are generally coated with hydrophobic ligands after the synthesis. Several methods have been developed for this and a recent review from Sedlmeier and Gorris gives an excellent overview on the topic[206].

Even though the synthesis methods have excellent control over particle size[207] and over size distribution[208], the issue of batch-to-batch variation remains as an issue[9]. The thermal decomposition method is perhaps the most common way of synthesizing e.g. the monodispersed $NaYF_4$-particles with excellent control over particle size[207–209]. This method is based on adding the organometallic precursors to a hot solvent that triggers their thermal decomposition and releases the reactants causing a rapid nucleation burst. The surface ligands coordinate to the growing particles and control their growth by blocking the expansion of the lattice[9]. The method however requires stringently controlled reaction temperatures, air-sensitive and expensive precursors, and an inert atmosphere. As the temperature range for the thermal decomposition is rather narrow (10 °C), it poses a significant challenge to the reproducibility[9].

2.4.2 Applications of upconverting phosphors in diagnostics

Applications in general

Upconverting phosphors have several features that make them an interesting label technology to be used in *in vitro* diagnostics. Features such as penetration depth of the NIR excitation[210], highly specific signal free from autofluorescence[211], resistance to photobleaching, non-blinking[212] narrow emission bands, large anti-Stokes shift, and long-lived luminescence are features that can be beneficial in the development of various types of assays.

UCPs were first utilized in a bioaffinity assay by Wright *et al* in 1997[213] when they were used as a label in a sandwich assay to detect Staphylococcal enterotoxin B. The first imaging applications emerged in 1999[214] when Zijlmans *et al* used UCPs as a marker for prostate specific antigen in tissue sections and CD4 membrane antigen on human lymphocytes. Van de Rijke *et al* reported a DNA array in 2001[215] that also demonstrated the superior sensitivity of UCPs compared to a Cy5 –label. All of these

studies utilized particles composed of $Y_2O_2S:Yb^{3+},Er^{3+}$ or Tm^{3+}, that would be considered rather bulky by current standards (200-400 nm in diameter).

Despite the crude materials, new applications were developed, such as a protein array by Lu *et al* in 2004[216] that utilized slightly smaller (80-150 nm) $NaYF_4:Yb^{3+},Er^{3+}$-particles, that had a magnetic core to demonstrate the preparation of multifunctional particles. Also a multianalyte immunoassay[217] and DNA genotyping[218] arrays have been reported using significantly smaller (25 nm in diameter) $NaYF_4:Yb^{3+},Er^{3+}$ – particles.

The first homogenous assays, based on energy transfer with the UCP-particle as a donor, were published almost simultaneously by two different groups in 2005. Wang *et al* reported a sandwich assay for avidin that was based on the quenching of the UCP emission through an energy transfer to gold nanoparticles[219] using 50 nm $NaYF_4:Yb^{3+},Er^{3+}$. Kuningas *et al*[220] on the other hand demonstrated the excitation of B-phycoerythrin through an UCP-particle in a competitive assay for biotin. These particles were bead-milled $La_2O_2S:Yb^{3+},Er^{3+}$ and $Y_2O_2S:Yb^{3+},Er^{3+}$ with an average diameter of 300 nm. This assay was further refined as an assay for the detection of estradiol in serum[221] and finally in whole blood[222]. Other examples of using UCPs as a donor in homogenous assays based on energy transfer include the detection of siRNA in live cells[223], enzyme activity assay[180] and a dual parameter sandwich assay for the detection of nucleic acids[224]. In addition to fluorescent proteins, gold, organic fluorophores, various acceptors, such as carbon nanoparticles[225], graphene oxide[226] and quantum dots[227] have been utilized in homogeneous assays with UCPs.

Chemical sensors are also a common way of utilizing UCPs and applications e.g. for sensing pH[228], carbon dioxide[229], ammonia[230], mercury[231], cyanide[232], temperature[233] and chromium[234] have been reported. UCPs have also been utilized in the monitoring of enzymatic reactions through the modulation of their emission with common cosubstrates and coenzymes[235,236]. Many of these applications take advantage of the several emission peaks of UCPs to provide an internal control signal and, instead of using a single emission intensity, calculate the ratiometric signal between two emission peaks.[230–233,236]

Applications in POC

Many of the homogeneous assays utilizing UCPs are already aimed at POC testing e.g. measurement in whole blood[51,222]. This is made possible by the penetration depth of the NIR-excitation and the transparency of whole blood[237] in the region where the red

emission of erbium can be used to excite an acceptor without any autofluorescence from the UCP excitation in the measurement window.

One analyte that is of a particular interest in POC is the measurement of glucose. It has traditionally been tested with test strips utilizing enzymes[238], but a general goal is to develop continuous glucose monitoring sensors[239]. With specific glucose binders, such as concanavalin A[240] and boronic acid derivatives[241], the development of also enzyme-free assays is possible. Competitive homogeneous assays for glucose have been developed with an UCP as a donor and graphene oxide[226] or gold nanoparticle[242] as a quencher. Both of these assays utilize 50 nm $NaYF_4$:Yb^{3+},Er^{3+}-particles and use the quencher to modulate the 547 nm emission of the UCP in human serum. Del Barrio *et al*[243] have constructed an enzyme-based sensor in a poly(acrylamide) film that uses a glucose oxidase cofactor flavin adenine dinucleotide to modulate the 475 nm emission of 26 nm $NaYF_4$:Yb^{3+},Tm^{3+}-particles, used to excite fluorescein linked to the glucose oxidase enzyme.

He and Liu[244] have utilized the homogenous assay principle of modulating the 547 nm emission of dendritic $NaYF_4$:Yb^{3+},Er^{3+} UCP-particles using a tetramethylrhodamine or a graphene oxide as an acceptor to attenuate the UCP emission. Their proof-of-concept assay detected the presence of matrix metalloproteinase-2 and carcinoembryonic antigen on a test strip composed of normal office paper. UCP proved to be an ideal photoluminescent label to be used with paper as the anti-Stokes detection circumvents the issue of high autofluorescence arising from fluorescent whitening agents in many commercial paper types.

The area of POC, where the highest number of applications for UCPs have been developed, is the lateral flow type of sandwich assays. This technology has been applied in the detection of circular anodic antigen[245,246], antibodies[247–250], bacteria[251–253], viruses[254], cytokines[248,255,256], and nucleic acids[12,13,250,257–261]. Comparison to an ELISA (enzyme-linked immunosorbent assay) has shown improved sensitivity[246,255] up to 100-fold[251]. Likewise comparison of UCP to colloidal gold on lateral flow assay has shown a 100-fold improvement[12]. Even though non-competitive assay format is often used, also competitive assay for drugs of abuse has been demonstrated[253]. For samples requiring pretreatment prior to detection with a lateral flow (LF) strip, various types of microfluidic devices have been combined with the LF strips[250,257–262], some of them specially designed for resource-poor settings, requiring no electricity[263,264].

When combined with a pre-amplification step with a PCR, a lateral flow assay with UCPs as a label has been able to detect human papillomavirus (HPV) DNA in a sample containing down to 2000 copies of HPV per 10 ng of total DNA. The sensitivity of the UCP-label made it possible to limit the number of PCR cycles to prevent artifacts arising from extended amplification.[12] The detection of infections without the amplification of DNA has also been studied with a detection limit of 10^6 bacterial cells.[13] This result is in line with a sandwhich assay for circular anodic antigen, that has a detection level between 10^5 and 10^6 target molecules per LF strip.[246]

Different ways of realizing a multianalyte assay with these tests have also been demonstrated. The most common method is, as usually for lateral flow assays, to use several test lines on a single strip[248,253,254,256]. As UCPs with different activator ions can be excited with a single excitation source, the use of two UCPs with different emission wavelengths has also been demontrated[265]. An interesting, and quite flexible, form of multiplexing was also to use a plastic holder to incorporate 10 lateral flow strips in order to simultaneously distribute a single sample to all of them[266].

Even though UCPs have been utilized in several lateral flow studies, very little attention has been paid to the particles themselves in these studies. A majority of the studies have used Y_2O_2S:Yb^{3+},Er^{3+}-particles[267] with an average diameter of 400 nm and $NaYF_4$:Yb^{3+},Er^{3+} with an average diameter of 250 nm[266]. Only one study has compared the large Y_2O_2S-particles to ten-fold smaller $NaYF_4$:Yb^{3+},Er^{3+} with a diameter of 40 nm in a lateral flow assay. The authors didn't find a significant difference between the performance of different particles and simply concluded that the smaller ones might be slightly better.[268]

2.4.3 Instrumentation for detecting UCPs

So far the lack of commercially available readers has been a significant drawback for UCPs and may have had a significant impact on the interest towards this technology. Gnach and Bednarkiewicz[16] have speculated that "The upconverting nanophosphors (UCNP) could have gained the same impact on biosciences as quantum dots had, if only the UCNPs could be accessible to broader bio-scientific community early enough, and, what is equally important, the commercial imaging instrumentation is available." A commercial reader called UpLink[269] from OraSure Technologies was briefly available, but has been discontinued. This device was classified as portable and equipped with a 1 W IR-laser for the excitation of the UCPs and a photomultiplier tube (PMT) for the detection. A Finnish company Labrox Oy has recently launched a

commercial instrument for UCP detection, named as the Upcon Reader. This is a multifunctional microtiter plate reader, equipped with a 2 W 976 nm laser and a photomultiplier tube, everything packed in the dimensions of 200 x 268 x 495 mm weighing 13 kg. It can also be equipped with a 10 W xenon flash lamp for the measurement of absorbance, luminescence, fluorescence, time-resolved fluorescence, and fluorescence polarisation in addition to upconversion

The advantage of quantum dots, mentioned by Gnach and Bednarkiewicz[16], is the ability to use existing instrumentation for fluorescence detection, equipped with a standard broadband excitation source such as xenon lamp. Ironically, the instrumentation needed for the detection of UCPs is rather simple and in some cases the NIR-radiation from a 75 W xenon-lamp has been sufficient, even though not optimal, for the excitation of larger (400 nm in diameter) UCPs[214,215]. In comparison to europium nanoparticles, there is no need for a temporal resolution, so pulsed excitation and time-gated detection are not necessary. Even though UCPs require a rather high excitation intensity (1-10^3 W/cm^2)[176] there are convenient, powerful and cheap InGaAs/AlGaAs/GaAs laser diodes available at the appropriate wavelength of around 980 nm.

So far many research groups have developed their own readers by adding a NIR laser diode to an existing plate reader[253], spectrometer[229], or microscope[265], together with the appropriate filters. In some cases the whole instrument has been custom built[267]. These readers commonly utilize a photomultiplier tube as a detector, combined with the NIR-laser with a power ranging from 0.05-1 W[253,267,269–271]. Soukka *et al*[270] have reported their reader of having an excitation intensity of over 40 W/cm^2. Based on the spot size from Huang *et al*[271], their instrument produced an intensity of 0.6 W/cm^2 with a 50 mW laser diode. For imaging a microarray in a microtiter well, Ylihärsilä *et al*[272] utilized a much more powerful laser with an output of 8 W and used a CCD-camera for the imaging of the anti-Stokes photoluminescence.

Lately, a Qiagen ESEQuant -device equipped with a laser and photodiodes has been used to detect UCPs from lateral flow strip[245]. Being impressively small (165 × 178 × 46 mm), lightweight (700 g), battery operated and indicating excellent field-robustness[248], this instrument is a promising demonstration how UCPs could be used even with hand-held readers. However, as photomultiplier tubes are the most sensitive detectors available, the use of a photodiode is a compromise between portability and sensitivity. Comparison to UpLink reader has revealed that the sensitivity of the ESEQuant is an order of magnitude lower than the one of UpLink reader[245].

3 AIMS OF THE STUDY

The overall aim of the study was to explore ways of utilizing time-resolved fluorescence and anti-Stokes detection in POC applications. The study was focused on the excitation wavelength of an Eu(III) ligand, suitable for bioaffinity assays, and on the use of upconverting phosphors as an internal light source in glucose sensing test strips and the modulation of their emission.

More specifically, the aims were:

I To develop a bioaffinity assay compatible enhancement solution for Eu(III) ions that would be excitable at wavelengths where high power light emitting diodes are available.

II To demonstrate the possibility of using upconverting phosphor particles as an internal light source in glucose sensing test strips.

III To study the feasibility of using UV-emitting, nanosized UCPs as an internal light source in glucose sensing test strip, and to compare their performance to the use of an external UV light source.

IV To study the use of microsized, visible emitting, upconverting phosphors as a signal amplifying component in a glucose sensing test strip by modulating their emission through the attenuation of the excitation and emission wavelengths.

4 SUMMARY OF MATERIALS AND METHODS

A detailed description of the materials and methods employed in this study can be found in the original publications (**I**-**IV**). A brief summary with some additional information is presented here.

4.1 Lanthanide labels

4.1.1 Enhancement solution for Eu(III)

The enhancement solution, that was studied in the original publication **I**, was based on the commercially available DELFIA enhancement solution (DES, Perkin-Elmer Life and Analytical Sciences - Wallac Oy, Turku, Finland)[273] with the light harvesting ligand replaced with a 9-ethyl-3,6-bis(5′,5′,5′,4′,4′-pentafluoro-1′,3′-dioxopentyl)carbazole (bdc, Figure 5 a). Its performance was compared against the original DELFIA solution that utilizes 2-naphthoyltrifluoroacetone (β-NTA, Figure 5 b) as the ligand.

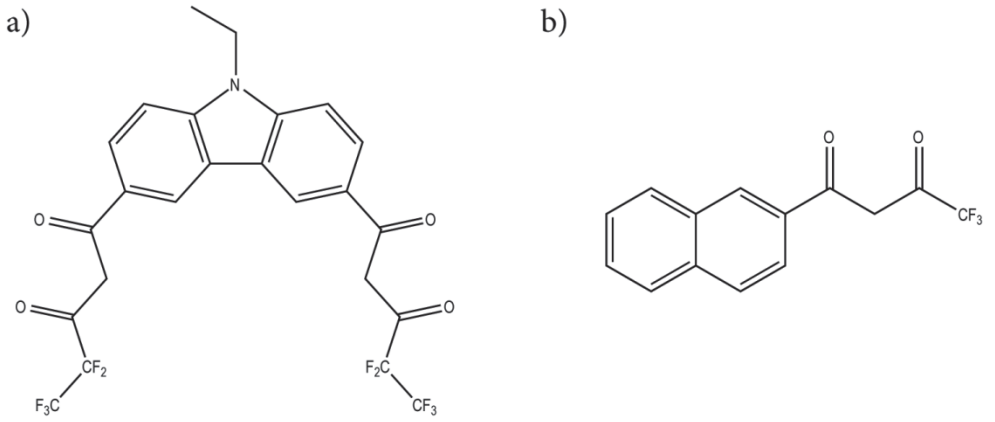

Figure 5. The structures of the light harvesting ligands used in the original publication **I**. **a)** the bdc-ligand and **b)** β-NTA-ligand used in the commercially available DELFIA Enhancement Solution, which was the point of comparison.

4.1.2 Upconverting phosphors

The UV-emitting upconverting nanophosphors (UCNPs) used in the original publications **II** and **III** were composed of β-$NaYF_4$:Yb^{3+},Tm^{3+}, synthesized in the

presence of K^+.[274] The commercial particles used in publications **II** and **IV** were upconverting microphosphors (UCμP) with Er(III) as the activator ion. These UCPs were purchased from Honeywell specialty chemicals GmbH (Seelze, Germany).

4.2 Reagent and strip preparation

4.2.1 Preparation of the enhancement solution

The composition of the bdc enhancement solution is based on that of the commercially available DELFIA Enhancement Solution, and was composed of 6.80 mM potassium hydrogen phthalate buffering solution (adjusted to pH 3.2 with acetic acid), containing 7.50 μM bdc, 50.0 μM trioctylphosphine oxide (TOPO) and 0.10% (v/v) Triton X-100. The solution was stored at +4 °C, protected from light.

4.2.2 Preparation of the glucose sensing test strips

The glucose sensing test strips were composed of two dry chemistry layers, coated on a plastic foil (Figure 6). The bottom layer contained the sensing components and the upper layer acted as a filter against the blood cells as well as a light reflecting layer. The UV-emitting UCNPs were located in the filtering (**II** and **III**) layer, and the VIS-emitting UCμPs in the sensing layer (**II** and **IV**).

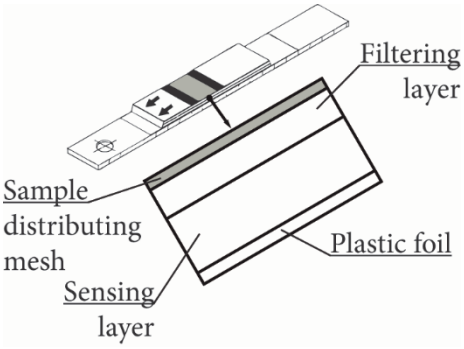

Figure 6. The structure of a glucose sensing test strip. The filtering layer prevents the blood cells from entering the sensing layer where they would interfere with the measurement. The sensing layer contains the components required for the enzymatic reaction and the indicator compound. The UCPs were located either in the filtering (**II** and **III**) or sensing layer (**II** and **IV**).

All of the strips were prepared by dissolving/suspending all of the components in mQ-water. Homogenous distribution was ensured by mechanical stirring, sonication and pressing the mixture through a fine mesh cloth. The final coatings were processed to a form of Accu-Chek® Active test strips shown in Figure 7.

Strips with the UV-emitting UCNPs

In the publications **II** and **III**, the composition of the strip sensing layer was as follows: Sensing layer: 101.1 g/L Sipernat FK 320DS (Evonik Industries AG, Hanau, Germany), 8.1 g/L poly(acrylic acid) (average molecular weight ~15 000, Sigma-Aldrich, Steinheim, Germany), 15.3 g/L Gantrez S-97 BF (Ashland, Marl, Germany), 40.4 g/L Propiofan 70D Propiofan 70D (BASF, Ludwigshafen, Germany), 1.6 g/L Geropon T77 (Rhodia, Milan, Italy), 64.7 g/L cNAD and 32.3 g/L glucose dehydrogenase (both from Roche Diagnostics GmbH, Penzberg, Germany) with pH adjusted to 7.5.

To incorporate the UCNPs in the filtering layer, the oleic acid, bound on the UCNP surface during the synthesis, was washed away with hydrochloric acid[275] to be replaced with the Gantrez-polymer. For this, the UCNP-particles were suspended to methanol with the polymer. After a uniform mixture was obtained, water was added and the pH adjusted with NaOH, until a homogenous suspension was formed. Methanol was then removed with a rotary evaporation to obtain the final concentrations of 65 g/L Gantrez and 300 g/L of UCNP. This mixture was then combined with the rest of the components for the filtering layer in the final concentrations of 411.6 g/L ZrO_2 TZ-3YS (Tosoh Corporation, Kaisei-cho, Japan), 8.7 g/L poly(acrylic acid), 54.1 g/L Propiofan 70D and 1 g/L Geropon T77.

To test the use of uncoated nano- and microsized particles in these test strips, either the $NaYF_4$:Yb^{3+},Tm^{3+} UCNP (with the oleic acid), or Honeywell UCμPs were embedded in the sensing layer. The UCPs were suspended in a aqueous suspension with poly(acrylic acid) in ratios (w/w) of 65 % UCP, 32 % water and 3 % poly(acrylic acid) without additional modifications.

The coating masses were then coated on the plastic film (Bayfol CR210, 125 μm thick, Bayer MaterialScience AG, Leverkusen, Germany) using a manual blade coating. The sensing layer was coated to a height of 75 μm and. After drying in +35 °C for 15 minutes, the second layer containing the UCNP was applied on top of this with a blade height of 100 μm and dried as the first one.

Strips with the VIS-emitting UCμPs

The strips used in the original publications **II** and **IV**, containing the commercial Honeywell UCμPs with the PMo indicator dye, were standard Accu-Chek® Active strips, made with coating mixtures obtained from Roche Diagnostics GmbH (Mannheim, Germany). The UCμPs were first suspended in a aqueous suspension with poly(acrylic acid) in ratios (w/w) of 65 % UCP, 32 % water and 3 % poly(acrylic acid) without additional modifications and then combined with the coating mass for the sensing layer. This mixture was then applied on the supporting plastic foil (corona treated yellow pokalon N 343 EM film, LOFO High Tech Film, Weil am Rhein, Germany) in a thickness of 158 μm by blade coating. After drying, the second mixture was applied in a thickness of 73 μm and dried.

4.3 Instrumentation

4.3.1 Time-resolved detection of the Eu(III) fluorescence

Time-resolved excitation and emission spectra as well as a fluorescence lifetime of 1 μM Eu(III) in DES and bdc-based solution (**I**) were measured with a Varian Cary spectrofluorometer using an excitation slit of 5 nm. The measurement delay and integration window were set to 100 and 600 μs, respectively. The lifetime of the 615 nm emission of Eu(III) in bdc-based solution was measured using either a 340 or 400 nm excitation wavelength, and the ligand concentration was varied between 5 and 40 μM. The lifetime of Eu(III) in DES was measured only with 340 nm excitation.

Eu(III) signal in the bio-BSA assay (**I**) was detected with a Victor^2 1420 multilabel counter (Perkin-Elmer Life and Analytical Sciences) using either a standard 340 or 365 nm (365/30 nm, Ferroperm, Denmark) excitation filter with a 400 μs measurement delay and a 400 μs window together with the standard 615 nm emission filter.

The molar absorptivities of the micellar complexes were calculated by measuring the absorbance of the complexed portion of the ligand in the enhancement solutions with 1 μM Eu(III) assuming that three ligand molecules are coordinated to one Eu(III) ion. The quantum yield of the micellar complex was determined according to the recommendations of IUPAC[276] using a DES-solution with 1.0 μM Eu(III) as a reference that has the known quantum yield of 0.70.[129] The lanthanide quantum

yields were determined as described by Xiao and Selvin[277] using sulforhodamine 101 as an acceptor in concentrations of 0.2, 0.6, and 1.0 μM.

4.3.2 Detection of the anti-Stokes photoluminescence of UCPs

The instrumentation used in the glucose assays (**II**-**IV**) was based on a Tidas S DAD -spectrometer (J&M Analytik AG, Essingen, Germany), equipped with a KG5 bandpass filter (FGS600, Thorlabs, Munich, Germany) in the emission light path. This instrument was used to detect either UCP emission or reflectance from the test strips. The UCPs were excited with a 100 mW NIR-laser (RLD-0980-PFR LabSpec 980 nm, Laserglow technologies, Toronto, Canada). The internal light source of the spectrometer was used for the measurement of reflectance in the original publications **II** and **III**. In the publication **IV**, it was replaced by a separate 50 W halogen lamp (LSB114/5, LOT-Oriel, Darmstadt, Germany) and an integrating sphere (K-050UV, LOT-Oriel) was used to collect the signal for the detector.

4.4 Assays

4.4.1 Bioaffinity assay for the comparison of Eu(III) enhancement solutions

The applicability of the bdc-based enhancement solution was demonstrated in a heterogeneous, noncompetitive assay for biotinylated bovine serum albumin (bio-BSA). A constant amount of Eu(III)-labeled streptavidin (Eu-SA) was used to detect different amounts of bio-BSA[278] on the bottom of SA-coated microtiter wells. Either bdc-based enhancement solution or DES was used for the detection of Eu-SA. Briefly, dilutions from 0.0032 to 625 ng/well of bio-BSA were first incubated in streptavidin coated wells. After the wells were washed, Eu(III) labeled streptavidin was added. After incubation, the wells were washed, and enhancement solutions were added. Finally, the signal from Eu(III) was measured using a time-resolved detection under a 340 or 365 nm excitation as described in section 4.3.1. Background signal was measured from a well that was not exposed to bio-BSA or Eu-SA, but contained the enhancement solution.

4.4.2 Glucose assay with UCPs

The measurement of blood glucose with test strips was based on an oxidoreductase enzyme embedded in the strip together with an indicator dye and the UCPs. The

enzyme oxidizes glucose to gluconolactone and the electron from this reaction is transferred to the indicator compound either directly (**II** and **III**), or via mediator compound (**II** and **IV**)[238]. This change in the oxidation state can then be observed as a change in the absorptivity that was used to attenuate the emission from the UCP-particles.

The UCP emission and the reflectance were both recorded at the range of 300-1000 nm. When comparing the UCP measurement with reflectance, the strips containing UCP were used with both methods. The spectrum was recorded initially from a dry strip without any sample to obtain the reference signal and, subsequently, after the addition of the 5 µL sample of either glucose in water (**II**-**IV**) or whole blood spiked with glucose (**II** and **III**).

The signal from the test strip (either UCP emission or reflectance) was analyzed as a relative signal. This was the percentage of the signal in the reaction endpoint, compared to the reference signal from the dry strip, before the addition of a sample. When using the UV-emitting UCNPs with cNAD as the indicator (**II** and **III**), the UV-emission (I_{UV} 330-380 nm) was normalized with the control signal (I_{ctrl} 440-490 nm) by integrating both of the emission peaks, and calculating a ratiometric signal of I_{UV}/I_{ctrl}. In the case of reflectance, intensity at 362 nm was used. With the Honeywell UCµPs with PMo as the indicator (**II** and **IV**), intensities at wavelengths 549 and 670 nm were used. In reflectance measurement, also the intensity at 978 nm was analyzed. The reaction endpoint was determined as a point on the kinetic curve where the slope was <2 %/s.

Two different configurations were used in the measurement of UCP emission from the test strips (Figure 7). With the UV-emitting UCNPs (**II** and **III**), the excitation source was located either below or above the test strip (Figure 7, both configurations). When using the Honeywell UCµPs (**II** and **IV**), the excitation source was always below the strip (Figure 7, left side). Reflectance was always measured with a broad band light being shined to the strip from below (Figure 7, left side).

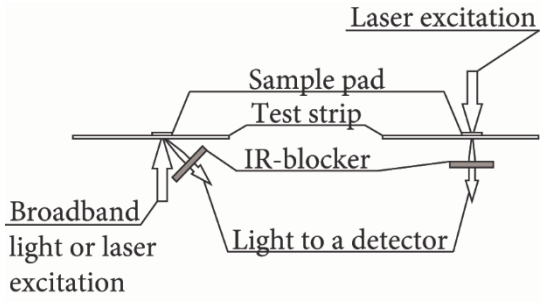

Figure 7. The configurations used when measuring reflectance and UCP emission from the glucose sensing test strips. On the left side a is setup used for all of the reflectance and UCP measurements and, on the right, a setup where the UV-emitting UCPs were excited through a layer of whole blood.

5 SUMMARY OF RESULTS AND DISCUSSION

5.1 Enhancement solution for Eu(III) ions (I)

5.1.1 Characterization of the enhancement solution

Excitation spectra of the europium chelates with the bdc-ligand from the original publication **I** (Figure 8) showed broad peaks in the 300–450 nm range, while DES has only one excitation peak at 340 nm from where the excitation efficiency decreases rapidly and is at the background level at 400 nm. The relative excitation efficiency of the bdc ligand in the 380–450 nm range compared to the 335 nm peak was affected by the concentration of the ligand. The excitation efficiency in this area increased with the increasing ligand concentration. There is no experimental data to explain what causes this, but we speculate that a high ligand concentration leads to a situation where a single ligand molecule participates in the chelation of only one Eu(III) ion whereas with lower ligand concentrations a single ligand may be attached to two separate ions.

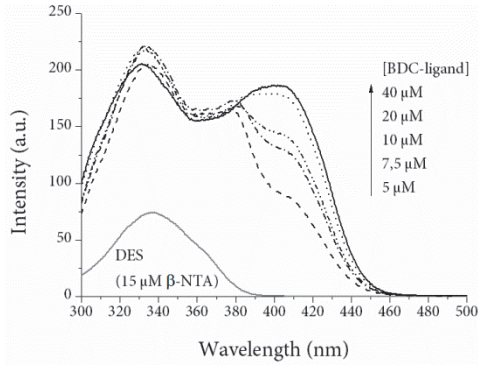

Figure 8. The excitation spectra of the enhancement solutions with a 5–40 µM bdc-ligand concentration and DES solution, both with 1 µM Eu(III). Different bdc-ligand concentrations are 5.0 µM (dash), 7.5 µM (dash dot), 10.0 µM (dash dot dot), 20.0 µM (dot), 40.0 µM (solid black), and DES (solid gray line). a.u., arbitrary unit.

The higher signal level of the bdc ligand complex was due to the molar absorptivities of the micellar complex, that at 340 nm, were on average 2.5 fold higher than the one of DES. As the ligand concentration in the enhancement solution is increased from 5 to 40 µM, the molar absorptivity at 405 nm rises from 44 000 to 68 000 $M^{-1}cm^{-1}$, respectively.

Quantum yields and fluorescence lifetimes of the micellar complex in different enhancement solutions with 1 µM Eu(III) produced almost identical results despite the enhancement solution used. The quantum yields with the bdc ligand concentrations from 5 to 20 µM ranged from 0.66 to 0.70, which is comparable to the one of DES (0.70). Bdc solution with a 40 µM ligand concentration was the exception with a lower quantum yield of 0.61. All of the bdc solutions had luminescence lifetimes between 738 and 757 µs that is practically the same measured for DES (743 µs). The excitation wavelength had no effect on the lifetime of the bdc enhancement solution, nor the relative emission intensities of the different Eu(III) emission peaks.

Due to a higher background signal in the bdc-solution, the lowest detectable concentration of Eu(III) was not improved compared to DES under a 340 nm excitation (Table 1). However, the wider excitation range made it possible to move the excitation up to 365 nm without compromising the limit of detection of the assay. In addition, the higher molar absorptivity of the bdc-ligand produced 3.0 times higher emission intensity when excited at 365 nm, compared to DES excited at 340 nm.

Table 1. Limits of detection and relative signal intensity for bio-BSA in the heterogenous assay using either DES of bdc-based enhancement solution when excited at 340 or 365 nm wavelength.

	Relative intensity		Limit of detection (fM)	
Enhancement solution	340 nm	365 nm	340 nm	365 nm
DES	1.0	0.4	32	190
7.5 µM bdc	2.5	3.0	64	63

5.1.2 Bioaffinity assay with europium label

The 7.5 µM bdc-ligand concentration was chosen to be used in the proof of principle – type of assay because it gave the highest signal with the plate reader (data not shown). In this heterogeneous assay, increasing the amount of bio-BSA in a microtitration well resulted in an increased binding of Eu(III) labeled streptavidin in a concentration dependent manner. Both enhancement solutions were able to produce a quantifiable (S/N > 3) signal from all the wells containing Eu(III)-SA, either due to the binding of Eu-SA through bio-BSA or a nonspecific binding. Using either DES with a 340 nm excitation or bdc-based enhancement solution with a 365 nm excitation resulted in the highest signal-to-noise (S/N) -ratios that were almost identical (Figure 9). This

indicates that the bdc-enhancement solution excited at 365 nm works equally well as DES excited at its optimal wavelength in the ligand binding assay.

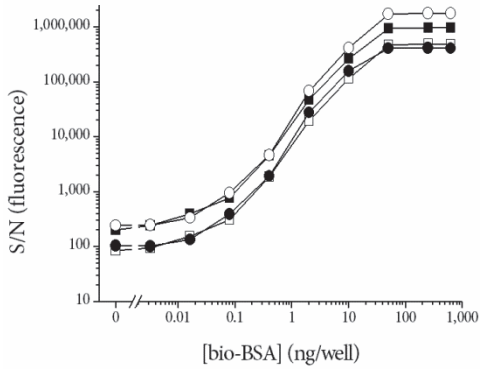

Figure 9. Signal-to-noise ratios obtained with the heterogeneous binding assay for biotinylated BSA using Eu(III)-labeled streptavidin as a tracer. The enhancement of Eu(III) was done by using either commercial DES or bdc-based enhancement solution. The different symbols represent DES with 340 nm excitation (filled squares), DES with 365 nm excitation (open squares), bdc with 340 nm excitation (filled circles), and bdc with 365 nm excitation (open circles).

5.2 UCP-particles as an internal light source (II-IV)

5.2.1 Reflectance of the test strips

The emission spectra of the different UCPs under 980 nm excitation, measured from dry glucose sensing test strips, are presented in Figure 10.

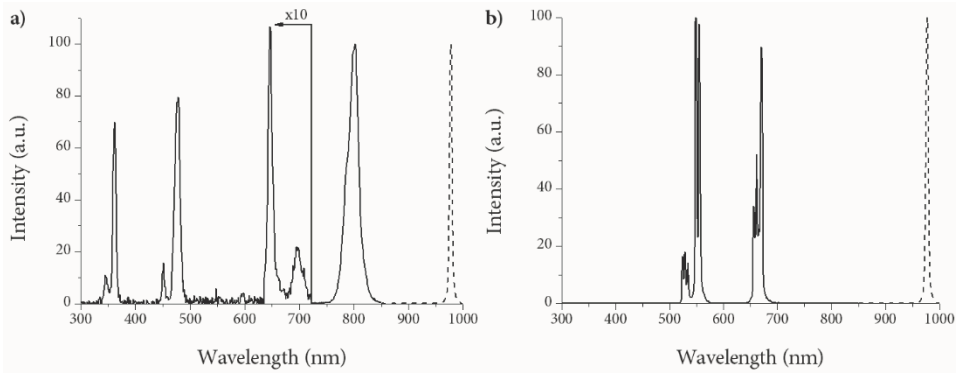

Figure 10. The upconversion emission spectra of the UCP-particles used in the original publications **II**-**IV**. **a)** Nanosized $NaYF_4$:Yb^{3+},Tm^{3+} (under a 2.4 W/cm^2 excitation) and **b)** commercially available microsized Honeywell Lumilux (under a 0.87 W/cm^2 excitation). The emission is presented with a solid line and the laser emission, used as an excitation source, plotted with a dashed line. a.u., arbitrary unit.

The two indicators used in the original publications **II**-**IV** were carba-nicotinamide adenine dinucleotide (cNAD)[279] and phosphomolybdenum blue (PMo, $H_6P_2Mo_{18}O_{62}$)[280]. The change in the test strip's reflectance, caused by these indicators after the addition of glucose, is presented in Figure 11.

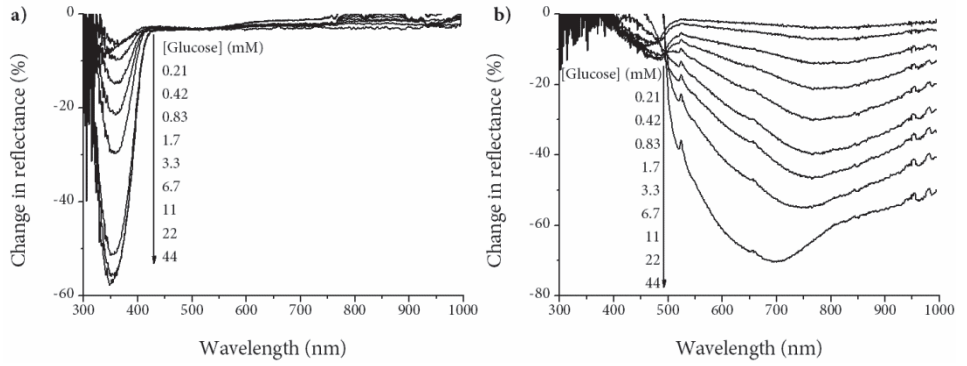

Figure 11. The change in the reflectance of a glucose sensing test strip as **a)** cNAD or **b)** PMo indicator dye is reduced after the introduction of glucose sample onto the strip.

5.2.2 Nanosized UV-emitting UCPs with cNAD as the indicator

In the original publications **II** and **III**, the glucose assay was based on an indicator dye that has a narrow absorption in the UV-region as a result of being reduced after the introduction of glucose on the test strip.

This assay was first tested by using a solution of glucose in water as a sample. The detection setup was based on the traditional configuration, having a light being shined to the test strip directly from the opposite side of sampling, and detecting the change in the reflection. For the measurement of the emission from upconverting nanophosphors (UCNPs), a broadband light source was replaced with a 980 nm laser, and the emission from the UCNPs was detected.

The results (Figure 12) obtained with different methods correlate well with the concentration of glucose in the sample if the internal control signal is used in the UCNP measurement. In terms of sensitivity and dynamic range, there is no noticeable difference between them. When the internal control of the UCNPs is omitted and only the UV-emission is used for the analysis, the standard deviations are significantly higher and the slope of the calibration curve lower. This is caused by the fluctuations in the UCNP-emission upon the addition of sample, caused by quenching, migration of the UCNPs in the test strip, and changes in the optical properties of the test strip.

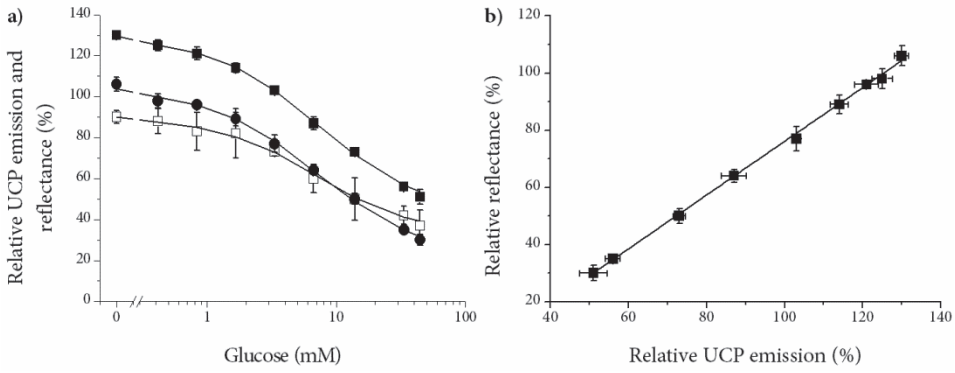

Figure 12. Results from the glucose assay with a light source below the strip and glucose dissolved in water as a sample. **a)** The glucose calibration curves obtained using either the emission of UCNPs (squares) or reflectance (spheres). The filled squares represent a ratiometric UCNP-signal and the open squares represent data obtained from the UV-emission of the UCNPs alone. The biexponential decay curve was used for the fitting. **b)** The correlation of the relative reflectance and ratiometric UCNP emission. The R^2 values of all the fittings were > 0.99. The error bars represent standard deviation from five replicate measurements.

To demonstrate the possibilities presented by the UCNPs to the design of optical setup, the excitation source was moved to the other side of the test strips and the assay repeated using a heparinized whole blood spiked with glucose as a sample. As human blood is relatively transparent for 980 nm radiation and the UCNPs provide an internal control signal, it was possible to measure the emission of UCNPs also in this

configuration. The same samples were then used also in a traditional reflectance based measurement to provide a point of comparison. Both measurements show a higher signal variation compared to the use of water and glucose as a sample, but the correlation between the two methods remains good (Figure 13).

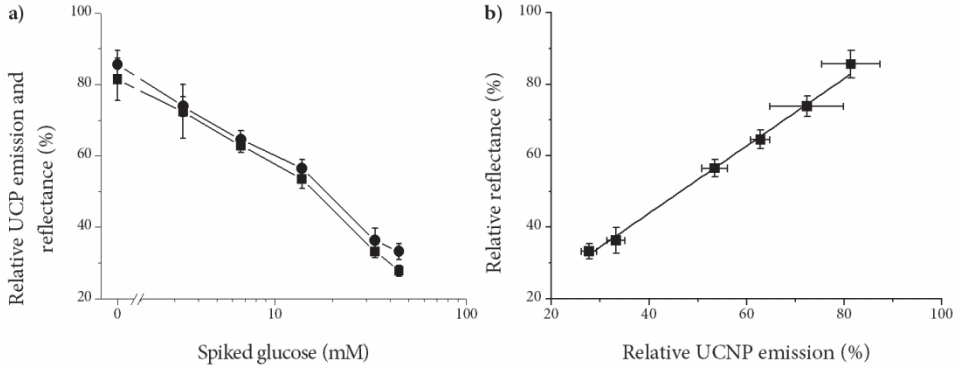

Figure 13. Results from the glucose assay with whole blood as sample. The UCNPs were excited through the sample and the reflectance was measured from the other side. **a)** The relative signals obtained from the UCNPs (squares) or reflectance (spheres) measurement. **b)** The correlation of the relative reflectance and ratiometric UCNP emission. R^2 of the linear fitting is >0.99. The error bars represent standard deviation from five replicate measurements.

5.2.3 Microsized, VIS-emitting UCP-particles as an internal light source with PMo indicator

In the original publications **II** and **IV**, the test strips had an indicator dye with a broad absorbance covering both the emission and the excitation range of the UCμPs.

The relative signals from the glucose measurement were plotted against the sample concentrations (Figure 14). The amplified response from the UCμPs in comparison to reflectance can be seen as a steeper calibration curve. This effect stems from the combined effect of filtering both emission and excitation wavelengths of the UCμPs. The relative signal ranges were almost doubled from 49 to 92 percentage points, when detecting the UCμP emission at 670 nm, compared to the measurement of reflectance at the respective wavelength. The slopes of the calibration curves at this wavelength were steepest at low glucose concentrations varying between 0.99-12 for the reflectance measurement and 1.1-36 for the UCμP measurement. It was also at the low glucose concentrations where the use of UCμPs made the highest improvement on the

slopes, up to three-fold. This difference decreases when the amount of glucose is increased and at 22 mM the slopes of the two methods are identical.

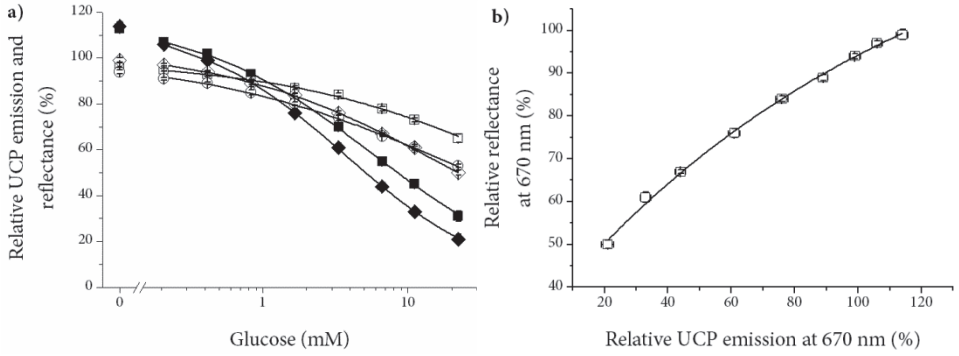

Figure 14. a) The relative signals obtained from the glucose assay by detecting either reflectance or UCμP emission. The filled symbols represent UCμP and the open ones reflectance measurement. The different wavelengths are denoted as squares, diamonds and circles for 549, 670 and 978 nm, respectively. **b)** The correlation of the relative reflectance and ratiometric UCμP emission. The R^2 values of all the fittings were > 0.99. The error bars represent standard deviation from ten replicate measurements.

5.2.4 Summary of UCP as an internal light source in glucose sensing test strips

Behavior of UCP particles in a test strip

The UV-emitting, nanosized $NaYF_4:Yb^{3+},Tm^{3+}$ particles produce enough emission for the signal to be quantified, but this required long integration times from the instrumentation used in this work. These UCNPs are also rather sensitive to the interaction with the water molecules resulting in quenching when an aqueous sample was introduced to the test strip. Coating the UCNPs with a high molecular weight polymer minimized this effect (Figure 15 a). In comparison, the significantly larger particles from Honeywell produce significantly higher emission and most of the signal was retained without a need for additional coating (Figure 15 b). These particles have an average diameter of 1.0 μm, but the composition is not reported by the manufacturer. However, based on the anti-Stokes emission spectrum it can be concluded that they use erbium as an activator ion. When the emission of the nanosized $NaYF_4:Yb^{3+},Tm^{3+}$ particles (average size 75*90 nm) was measured from a test strip before and after the addition of water, the intensity of the detected signal went down by 78-96 % (depending on the wavelength). After the particles were coated with the high molecular weight Gantrez-polymer, the signal decrease was only 14-30 % (Figure 15 a). When the UCNPs in the strips were replaced with larger ones from

Honeywell, the signal decrease upon the addition of water was only 30 % (at 550-670 nm, Figure 15 b). This result is identical to the one obtained with polymer coated nanosized UCNPs at 646 nm. This decrease in the signal is most likely due to optical properties of the strip changing upon wetting.

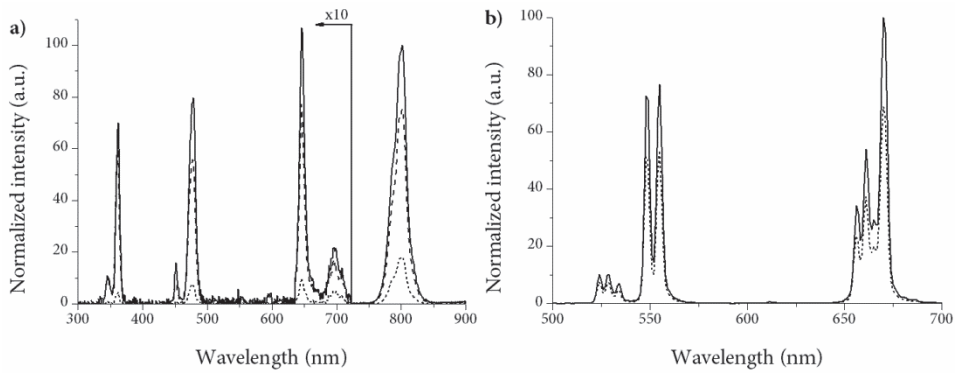

Figure 15. The UCP emission spectra recorded from the test strip before (solid line) and after (dotted line) the addition of sample of water. **a)** Nanosized $NaYF_4$:Yb^{3+},Tm^{3+} particles (under a 2.4 W/cm^2 excitation) are heavily quenched by water when not protected by a polymer, which minimizes this effect (dashed line). **b)** The larger particles from Honeywell (under a 0.87 W/cm^2 excitation) show a similar decrease in the signal as the polymer coated UCNPs without any additional modification. a.u., arbitraty unit.

Assay performance

The results from the glucose assays using different particles and different strips (**II**-**IV**) are compared to the respective reflectance measurement in Table 2. In both cases the use of UCPs as an internal light source on glucose sensing test strips lead to an improvement in the limit of detection, which was roughly two-fold lower than the one obtained with a reflectance measurement. With the larger Honeywell UCμPs, modulating the emission by attenuating the excitation lead also to a steeper calibration curve. However, the signal variation with the UCμPs is higher than with reflectance, but still significantly better than the CV% (coefficient of variation) in the measurement with the UV-emitting UCNPs, when the internal control signal is omitted. This indicates that the larger UCPs provide a more stable signal in the test strip than the nanosized ones.

Table 2. Summary of the results from using UCPs as an internal light source in glucose sensing test strips.

	UV-emitting UCNPs ($NaYF_4$:Yb^{3+},Tm^{3+}) with cNAD indicator		VIS-emitting UCμPs (unknown composition with Er^{3+}) with PMo indicator	
Detection method	Reflectance	UCNP emission	Reflectance	UCP emission
Indicator absorbance	Narrow 361 nm (FWHM ~40 nm)[279]		Broad ~550 to over 1000 nm	
Detected wavelength	362 nm	362 nm and 478 nm[a]	670 nm	
Limit of detection	930 μM	490 μM	11.9 μM	5.7 μM
CV%	0.92-9.1	0.64-6.7 (2.9-21)[b]	0.63-2.1	0.95-9.4
Slope of the calibration curve	0.61-12	0.66-11	0.99-12	1.1-36

[a] 362 nm was attenuated by the indicator dye and 478 nm was used as an internal control signal.

[b] The variation of the CV% when the internal control signal is not used in the analysis.

6 CONCLUSIONS

Point-of-care –diagnostics is a rapidly growing segment of *in vitro* diagnostics with a pressure to push the performance of the assays constantly further. As the benefits of lanthanide photoluminescence have been well established in several diagnostic applications, it might well be a useful tool also in the improvement of POC assays.

In this thesis, ways of utilizing time-resolved and anti-Stokes detection in POC were explored. Time-resolved fluorometry was studied by developing a novel enhancement solution for Eu(III)-ions that would be applicable in bioaffinity assays. Anti-Stokes detection was utilized by using upconverting phosphors as an internal light source in blood glucose sensing test strips.

The main conclusions based on the original publications are presented below.

I An enhancement solution based on a novel light harvesting ligand enabled the efficient excitation of Eu(III)-ions and produced a high signal in a bioaffinity assay. The new enhancement solution was also excitable in the wavelength range where high power light emitting diodes are available. The high emission intensity, produced by the ligand, is beneficial when attempting to overcome the limitations brought by the low excitation power and detection sensitivity of miniaturized components essential for various POC devices.

II Different kind of upconverting phosphors were found to be a feasible alternative to be used as an internal light source in glucose sensing test strips. The modulation of the detected UCP emission with a redox-indicator compound was found to be an alternative way of detecting glucose in sample solution and several wavelengths of the UCPs could be utilized for this purpose.

III UV-emitting UCNPs could be used as an internal light source in glucose-sensing dry chemistry test strips to replace an external UV light source with a NIR-laser. They also provided an additional degree of freedom on the design of the optical setup of the instrumentation. The results were comparable to a commonly used reflectance measurement.

IV The use of VIS-emitting UCμPs as an internal light source in glucose sensing test strips, together with a broad absorbing redox-indicator provided a way of

manipulating the slope of the assay calibration curve. By utilizing the non-linear relationship between the excitation power and the emission intensity of the UCμPs, they can be used as a signal-amplifying component for a NIR-absorbing indicator dye.

As discussed in the literary review, the lack of compact instrumentation is a considerable obstacle in the use of lanthanide labels in POC applications. However, the research with the UCPs has been focused on producing increasingly smaller particles and it seems that the potential of larger crystals has been somewhat overlooked, as there does not seem to be well-established methods of synthesizing monodisperse particles with a diameter of over 200 nm. As larger particles have higher luminescence output and might be suitable for various applications, they could be an important factor in bringing upconversion to POC applications.

ACKNOWLEDGEMENTS

This study was carried out in the Department of Biotechnology, University of Turku and in Roche Diagnostics GmbH, Diabetes Care, in Mannheim, Germany during the years 2010-2015. The work was supported by the European Union under the initial training network for chemical bioanalysis (ITN CHEBANA) and by the doctoral programme in molecular life sciences of the University of Turku.

During this time, I have had the great privilege of working with highly skilled professionals both in the University of Turku and in Roche Diagnostics. I wish to express my deepest gratitude to Professor Tero Soukka, Dr Carina Horn and Dr Bernd Schneidinger for all of their contributions to this thesis. I am also especially grateful to Dr Nelli Steinke and Dr Andreas Weller for sharing their invaluable knowledge about glucose measurement.

I would like to thank Dr Harri Hakala and Dr Thomas Hirsch for taking time and reviewing this thesis. Their comments and feedback were invaluable and helped to improve this work. I also greatly appreciate the work of Maria Tyystjärvi who, as the official "comma filer", reviewed the language of this thesis.

None of the publications would have been possible without the work from the co-authors Professor Jouko Kankare, Dr Iko Hyppänen, Dr Harri Takalo, Vishal Kale, Eeva-Maija Puputti and the patent experts of Roche Diagnostics, Sabine Grau and Dr Karsten Riwotzki.

I also wish to thank several colleagues and co-workers I have had the honour of working with during these years. First and foremost this goes to all the people in Roche Diabetes Care. I quickly came to realize that the Roche slogan, "Great place to work", was very true. You provided a pleasant atmosphere and made me feel very welcome. You also had a great deal of patience when I started switching from English to German and bravely gave me a chance to practise my language skills. Es war eine Ehre und Freude mit euch zu arbeiten. Vielen herzlichen Dank! Nevertheless it was great to have Maksim Fomin there to provide a whole lot of peer support as another foreign PhD student in the lab and Anna Ahomaa, my self-proclaimed "finnish little sister in Germany". The other international reinforcements, Joachim and Prosper along with the other members of the GoCARB project, provided some interesting and, from time to time, downright disturbing lunch conversations. It was also a great

pleasure to share an office with Dr Johannes Graf. You were an invaluable help in countless occasions, not to mention a great company together with Riikka and Matti.

The CHEBANA programme provided a memorable network and I wish to thank Dr Heike Mader who was always there to provide answers to my endless questions. This network also made it possible to visit some great places including Regensburg and Compiègne. All of the PhD students and postdocs in CHEBANA made our meetings memorable and I always looked forward to them. Thomas Zanni and my other "amici Italiani" greatly improved my language skills, although the vocabulary was rather limited. Now I should proceed to learn also some non-profanities in Italian.

Despite all the places visited during this work, Turku is still the one I call home and it wouldn't be that without the people in the Department of Biotechnology. There are numerous people with whom I have shared many moments in the break room and in the lab. Most importantly everyone who has been working in LEAP/INFRA/UpCon etc… projects during these years. Riikka Arppe in particular was a valuable contact for keeping me up-to-date with all the gossip when I was in Germany and for providing consultation in several work-related issues.

Finally, the biggest thanks goes to my lovely soon-to-be wife Venla. Thank you for not arguing too much when I got the idea to go to Germany (Professor Soukka is the one to blame for that) and for putting up with everything that came with it. It has been a unique experience for both of us and now you can finally call yourself "tohtorinna".

Turku, August 2015

Timo Valta

REFERENCES

1. Ryan, F., O'Shea, S. & Byrne, S. The 'carry-over' effects of patient self-testing: Positive effects on usual care management by an anticoagulation management service. *Thromb. Res.* **126,** e345–e348 (2010).

2. Price, C. P. Point of care testing. *BMJ* **322,** 1285–1288 (2001).

3. Laurence, C. O., Moss, J. R., Briggs, N. E. & Beilby, J. J. The cost-effectiveness of point of care testing in a general practice setting: results from a randomised controlled trial. *BMC Health Serv. Res.* **10,** 165 (2010).

4. Hamad, M. A. S., Eekelen, E. van, Agt, T. van & Straten, A. H. M. van. Self-management program improves anticoagulation control and quality of life: a prospective randomized study. *Eur. J. Cardiothorac. Surg.* **35,** 265–269 (2009).

5. Gadisseur, A. P. A., Breukink-Engbers, W. G. M., van der Meer, F. J. M., van den Besselaar, A. M. H., Sturk, A. & Rosendaal, F. R. Comparison of the quality of oral anticoagulant therapy through patient self-management and management by specialized anticoagulation clinics in the netherlands: A randomized clinical trial. *Arch. Intern. Med.* **163,** 2639–2646 (2003).

6. Rebel, A., Rice, M. A. & Fahy, B. G. The Accuracy of Point-of-Care Glucose Measurements. *J. Diabetes Sci. Technol.* **6,** 396–411 (2012).

7. Kuswandi, B., Nuriman, Huskens, J. & Verboom, W. Optical sensing systems for microfluidic devices: A review. *Anal. Chim. Acta* **601,** 141–155 (2007).

8. Bünzli, J.-C. G. & Piguet, C. Taking advantage of luminescent lanthanide ions. *Chem. Soc. Rev.* **34,** 1048 (2005).

9. DaCosta, M. V., Doughan, S., Han, Y. & Krull, U. J. Lanthanide upconversion nanoparticles and applications in bioassays and bioimaging: A review. *Anal. Chim. Acta* **832,** 1–33 (2014).

10. Juntunen, E., Myyryläinen, T., Salminen, T., Soukka, T. & Pettersson, K. Performance of fluorescent europium(III) nanoparticles and colloidal gold reporters in lateral flow bioaffinity assay. *Anal. Biochem.* **428,** 31–38 (2012).

11. Zhang, F., Zou, M., Chen, Y., Li, J., Wang, Y., Qi, X. & Xue, Q. Lanthanide-labeled immunochromatographic strips for the rapid detection of Pantoea stewartii subsp. stewartii. *Biosens. Bioelectron.* **51,** 29–35 (2014).

12. Corstjens, P., Zuiderwijk, M., Brink, A., Li, S., Feindt, H., Niedbala, R. S. & Tanke, H. Use of Up-Converting Phosphor Reporters in Lateral-Flow Assays to Detect Specific Nucleic Acid Sequences: A Rapid, Sensitive DNA Test to Identify Human Papillomavirus Type 16 Infection. *Clin. Chem.* **47,** 1885–1893 (2001).

13. Zuiderwijk, M., Tanke, H. J., Sam Niedbala, R. & Corstjens, P. L. A. M. An amplification-free hybridization-based DNA assay to detect Streptococcus pneumoniae utilizing the up-converting phosphor technology. *Clin. Biochem.* **36,** 401–403 (2003).

14. Liu, J., Du, B., Zhang, P., Haleyurgirisetty, M., Zhao, J., Ragupathy, V., Lee, S., DeVoe, D. L. & Hewlett, I. K. Development of a microchip Europium nanoparticle immunoassay for sensitive point-of-care HIV detection. *Biosens. Bioelectron.* **61,** 177–183 (2014).

15. Rundström, G., Jonsson, A., Mårtensson, O., Mendel-Hartvig, I. & Venge, P. Lateral Flow Immunoassay Using Europium (III) Chelate Microparticles and Time-Resolved Fluorescence for Eosinophils and Neutrophils in Whole Blood. *Clin. Chem.* **53,** 342–348 (2007).

16. Gnach, A. & Bednarkiewicz, A. Lanthanide-doped up-converting nanoparticles: Merits and challenges. *Nano Today* **7,** 532–563 (2012).

17. Bui, D. A. & Hauser, P. C. Analytical devices based on light-emitting diodes – a review of the state-of-the-art. *Anal. Chim. Acta* **853,** 46–58 (2015).

18. Park, H. M. & Joo, K. S. Performance characteristics of a silicon photomultiplier based compact radiation detector for Homeland Security applications. *Nucl. Instrum. Methods Phys. Res. A* **781,** 1–5 (2015).

19. Bünzli, J.-C. G. On the design of highly luminescent lanthanide complexes. *Coord. Chem. Rev.* (2014). doi:10.1016/j.ccr.2014.10.013

20. Chen, G., Ågren, H., Ohulchanskyy, T. Y. & Prasad, P. N. Light upconverting core–shell nanostructures: nanophotonic control for emerging applications. *Chem Soc Rev* **44,** 1680–1713 (2015).

21. Owens, D. R. History and Vision: What is Important for Patients with Diabetes? *Diabetes Technol. Ther.* **10,** S–5 (2008).

22. Luntz, G. A Simple Quick Test for Glucose in Urine. *BMJ* **1,** 499–500 (1957).

23. Free, A. H. & Free, H. M. Self testing, an emerging component of clinical chemistry. *Clin. Chem.* **30,** 829–838 (1984).

24. Mazzaferri, E., Lanese, R., Skillman, T. & Keller, M. Use of test strips with colour meter to measure blood-glucose. *The Lancet* **295,** 331–333 (1970).

25. Lowy, C. Home glucose monitoring, who started it? *BMJ* **316,** 1467 (1998).

26. Ehrenkranz, J. R. L. Home and Point-of-Care Pregnancy Tests: A Review of the Technology. *Epidemiology* **13,** S15–S18 (2002).

27. Point of Care Diagnostics. at <http://www.bccresearch.com/market-research/healthcare/point-of-care-diagnostics-hlc043d.html>

28. WHO | Mapping the landscape of diagnostics for sexually transmitted infections. *WHO* at <http://www.who.int/tdr/publications/tdr-research-publications/mapping-landscape-sti/en/>

29. Huppert, J., Hesse, E. & Gaydos, C. A. What's the Point? How Point-of-Care STI Tests Can Impact Infected Patients. *Point Care* **9,** 36–46 (2010).

30. Schito, M., Peter, T. F., Cavanaugh, S., Piatek, A. S., Young, G. J., Alexander, H., Coggin, W., Domingo, G. J., Ellenberger, D., Ermantraut, E., Jani, I. V., Katamba, A., Palamountain, K. M., Essajee, S. & Dowdy, D. W. Opportunities and Challenges for Cost-Efficient Implementation of New Point-of-Care Diagnostics for HIV and Tuberculosis. *J. Infect. Dis.* **205,** S169–S180 (2012).

31. Chin, C. D., Linder, V. & Sia, S. K. Lab-on-a-chip devices for global health: Past studies and future opportunities. *Lab. Chip* **7,** 41–57 (2007).

32. Luppa, P. B., Müller, C., Schlichtiger, A. & Schlebusch, H. Point-of-care testing (POCT): Current techniques and future perspectives. *TrAC Trends Anal. Chem.* **30,** 887–898 (2011).

33. Gubala, V., Harris, L. F., Ricco, A. J., Tan, M. X. & Williams, D. E. Point of care diagnostics: status and future. *Anal. Chem.* **84,** 487–515 (2012).

34. Soper, S. A., Brown, K., Ellington, A., Frazier, B., Garcia-Manero, G., Gau, V., Gutman, S. I., Hayes, D. F., Korte, B., Landers, J. L., Larson, D., Ligler, F., Majumdar, A., Mascini, M., Nolte, D., Rosenzweig, Z., Wang, J. & Wilson, D. Point-of-care biosensor systems for cancer diagnostics/prognostics. *Biosens. Bioelectron.* **21,** 1932–1942 (2006).

35. Gervais, L., de Rooij, N. & Delamarche, E. Microfluidic Chips for Point-of-Care Immunodiagnostics. *Adv. Mater.* **23,** H151–H176 (2011).

36. Mohammed, M.-I. & Desmulliez, M. P. Y. Lab-on-a-chip based immunosensor principles and technologies for the detection of cardiac biomarkers: a review. *Lab Chip* **11,** 569–595 (2011).

37. Myers, F. B. & Lee, L. P. Innovations in optical microfluidic technologies for point-of-care diagnostics. *Lab. Chip* **8,** 2015–2031 (2008).

38. Singh, J., Sharma, S. & Nara, S. Evaluation of gold nanoparticle based lateral flow assays for diagnosis of enterobacteriaceae members in food and water. *Food Chem.* **170,** 470–483 (2015).

39. Ali, M. E., Hashim, U., Mustafa, S., Che Man, Y. B. & Islam, K. N. Gold Nanoparticle Sensor for the Visual Detection of Pork Adulteration in Meatball Formulation. *J. Nanomater.* **2012,** e103607 (2011).

40. Liu, G., Mao, X., Phillips, J. A., Xu, H., Tan, W. & Zeng, L. Aptamer-nanoparticle strip biosensor for sensitive detection of cancer cells. *Anal. Chem.* **81,** 10013–10018 (2009).

41. Zhang, C., Zhang, Y. & Wang, S. Development of Multianalyte Flow-through and Lateral-Flow Assays Using Gold Particles and Horseradish Peroxidase as Tracers for the Rapid Determination of Carbaryl and Endosulfan in Agricultural Products. *J. Agric. Food Chem.* **54,** 2502–2507 (2006).

42. Yang, W., Li, X., Liu, G., Zhang, B., Zhang, Y., Kong, T., Tang, J., Li, D. & Wang, Z. A colloidal gold probe-based silver enhancement immunochromatographic assay for the rapid detection of abrin-a. *Biosens. Bioelectron.* **26,** 3710–3713 (2011).

43. Sajid, M., Kawde, A.-N. & Daud, M. Designs, formats and applications of lateral flow assay: A literature review. *J. Saudi Chem. Soc.* doi:10.1016/j.jscs.2014.09.001

44. Freckmann, G., Schmid, C., Baumstark, A., Pleus, S., Link, M. & Haug, C. System Accuracy Evaluation of 43 Blood Glucose Monitoring Systems for Self-Monitoring of Blood Glucose according to DIN EN ISO 15197. *J. Diabetes Sci. Technol.* **6,** 1060–1075 (2012).

45. Reyes, D. R., Iossifidis, D., Auroux, P.-A. & Manz, A. Micro total analysis systems. 1. Introduction, theory, and technology. *Anal. Chem.* **74,** 2623–2636 (2002).

46. Hata, K., Kichise, Y., Kaneta, T. & Imasaka, T. Hadamard transform microchip electrophoresis combined with diode laser fluorometry. *Anal. Chem.* **75,** 1765–1768 (2003).

47. Aubin, J. E. Autofluorescence of viable cultured mammalian cells. *J. Histochem. Cytochem.* **27,** 36–43 (1979).

48. Wang, S. C. & Morris, M. D. Plastic microchip electrophoresis with analyte velocity modulation. Application to fluorescence background rejection. *Anal. Chem.* **72,** 1448–1452 (2000).

49. Soini, E. & Hemmilä, I. Fluoroimmunoassay: present status and key problems. *Clin. Chem.* **25,** 353–361 (1979).

50. Mariella, R. Sample preparation: the weak link in microfluidics-based biodetection. *Biomed. Microdevices* **10,** 777–784 (2008).

51. Arppe, R., Mattsson, L., Korpi, K., Blom, S., Wang, Q., Riuttamäki, T. & Soukka, T. Homogeneous Assay for Whole Blood Folate Using Photon Upconversion. *Anal. Chem.* **87,** 1782–1788 (2015).

52. Wabuyele, M. B., Ford, S. M., Stryjewski, W., Barrow, J. & Soper, S. A. Single molecule detection of double-stranded DNA in poly(methylmethacrylate) and polycarbonate microfluidic devices. *Electrophoresis* **22,** 3939–3948 (2001).

53. Ivaska, L., Niemelä, J., Heikkinen, T., Vuorinen, T. & Peltola, V. Identification of respiratory viruses with a novel point-of-care multianalyte antigen detection test in children with acute respiratory tract infection. *J. Clin. Virol.* **57,** 136–140 (2013).

54. Owens, C. V., Davidson, Y. Y., Kar, S. & Soper, S. A. High-Resolution Separation of DNA Restriction Fragments Using Capillary Electrophoresis with Near-IR, Diode-Based, Laser-Induced Fluorescence Detection. *Anal. Chem.* **69,** 1256–1261 (1997).

55. Petty, H. R., Elner, V. M., Kawaji, T., Clark, A., Thompson, D. & Yang, D.-L. A facile method for immunofluorescence microscopy of highly autofluorescent human retinal sections using nanoparticles with large Stokes shifts. *J. Neurosci. Methods* **191,** 222–226 (2010).

56. Hawkins, K. R. & Yager, P. Nonlinear decrease of background fluorescence in polymer thin-films - a survey of materials and how they can complicate fluorescence detection in μTAS. *Lab. Chip* **3,** 248–252 (2003).

57. Tu, D., Zheng, W., Liu, Y., Zhu, H. & Chen, X. Luminescent biodetection based on lanthanide-doped inorganic nanoprobes. *Coord. Chem. Rev.* **273–274,** 13–29 (2014).

58. Hagan, A. K. & Zuchner, T. Lanthanide-based time-resolved luminescence immunoassays. *Anal. Bioanal. Chem.* **400,** 2847–2864 (2011).

59. Hans Wedepohl, K. The composition of the continental crust. *Geochim. Cosmochim. Acta* **59,** 1217–1232 (1995).

60. Balachandran, G. in *Ind. Process.* (ed. Seetharaman, S.) **3,** 1291–1340 (Elsevier, 2014).

61. Binnemans, K., Jones, P. T., Blanpain, B., Van Gerven, T. & Pontikes, Y. Towards zero-waste valorisation of rare-earth-containing industrial process residues: a critical review. *J. Clean. Prod.* (2015). doi:10.1016/j.jclepro.2015.02.089

62. Hao, Z., Li, Y., Li, H., Wei, B., Liao, X., Liang, T. & Yu, J. Levels of rare earth elements, heavy metals and uranium in a population living in Baiyun Obo, Inner Mongolia, China: A pilot study. *Chemosphere* **128,** 161–170 (2015).

63. Freeman, A. J. & Watson, R. E. Theoretical Investigation of Some Magnetic and Spectroscopic Properties of Rare-Earth Ions. *Phys. Rev.* **127,** 2058–2075 (1962).

64. Werts, M. H. V. Making sense of lanthanide luminescence. *Sci. Prog.* **88,** 101–131 (2005).

65. Ling, L. & Wang, N.-H. L. Ligand-assisted elution chromatography for separation of lanthanides. *J. Chromatogr. A* **1389,** 28–38 (2015).

66. D'Aléo, A., Pointillart, F., Ouahab, L., Andraud, C. & Maury, O. Charge transfer excited states sensitization of lanthanide emitting from the visible to the near-infra-red. *Coord. Chem. Rev.* **256,** 1604–1620 (2012).

67. Bünzli, J.-C. G. & Eliseeva, S. V. in *Lanthan. Lumin.* (eds. Hänninen, P. & Härmä, H.) 1–45 (Springer Berlin Heidelberg, 2010).

68. Carnall, W. T. in *Handb. Phys. Chem. Rare Earths* (eds. Gschneidner, K. A. J. & Eyring, L.) **3,** 171–208 (Elsevier, 1979).

69. Russell, H. N. & Saunders, F. A. New Regularities in the Spectra of the Alkaline Earths. *Astrophys. J.* **61,** 38–69 (1925).

70. Weissman, S. I. Intramolecular Energy Transfer The Fluorescence of Complexes of Europium. *J. Chem. Phys.* **10,** 214–217 (1942).

71. Wieder, I. in *Immunofluoresc. Relat. Stain. Tech.* (eds. Knapp, W., Holubar, K. & Wick, G.) 67–80 (Elsevier, 1978).

72. Siitari, H., Hemmilä, I., Soini, E., Lövgren, T. & Koistinen, V. Detection of hepatitis B surface antigen using time-resolved fluoroimmunoassay. *Nature* **301,** 258–60 (1983).

73. Bünzli, J.-C. G. Lanthanide Luminescence for Biomedical Analyses and Imaging. *Chem. Rev.* **110,** 2729–2755 (2010).

74. Armelao, L., Quici, S., Barigelletti, F., Accorsi, G., Bottaro, G., Cavazzini, M. & Tondello, E. Design of luminescent lanthanide complexes: From molecules to highly efficient photo-emitting materials. *Coord. Chem. Rev.* **254,** 487–505 (2010).

75. Sabbatini, N., Guardigli, M. & Lehn, J.-M. Luminescent lanthanide complexes as photochemical supramolecular devices. *Coord. Chem. Rev.* **123,** 201–228 (1993).

76. Räsänen, M., Takalo, H., Rosenberg, J., Mäkelä, J., Haapakka, K. & Kankare, J. Study on photophysical properties of Eu(III) complexes with aromatic β-diketones – Role of charge transfer states in the energy migration. *J. Lumin.* **146,** 211–217 (2014).

77. Piguet, C. & Bünzli, J.-C. G. in *Handb. Phys. Chem. Rare Earths* (eds. Gschneidner, K. A. J., Bünzli, J.-C. G. & Pecharsky, V. K.) **40,** 301–553 (Elsevier, 2010).

78. Jin, D., Connally, R. & Piper, J. Long-lived visible luminescence of UV LEDs and impact on LED excited time-resolved fluorescence applications. *J. Phys. Appl. Phys.* **39,** 461–465 (2006).

79. Dickson, E. F., Pollak, A. & Diamandis, E. P. Time-resolved detection of lanthanide luminescence for ultrasensitive bioanalytical assays. *J. Photochem. Photobiol. B* **27,** 3–19 (1995).

80. Kuusisto, A. & Hänninen, P. in *Lanthan. Lumin.* (eds. Hänninen, P. & Härmä, H.) 263–277 (Springer Berlin Heidelberg, 2011).

81. Steemers, F. J., Verboom, W., Reinhoudt, D. N., van der Tol, E. B. & Verhoeven, J. W. New Sensitizer-Modified Calix[4]arenes Enabling Near-UV Excitation of Complexed Luminescent Lanthanide Ions. *J. Am. Chem. Soc.* **117,** 9408–9414 (1995).

82. Latva, M., Takalo, H., Simberg, K. & Kankare, J. Enhanced Eu^{III} ion luminescence and efficient energy transfer between lanthanide chelates within the polymeric structure in aqueous solutions. *J. Chem. Soc. Perkin Trans. 2* 995–999 (1995).

83. Van der Tol, E. B., van Ramesdonk, H. J., Verhoeven, J. W., Steemers, F. J., Kerver, E. G., Verboom, W. & Reinhoudt, D. N. Tetraazatriphenylenes as Extremely Efficient Antenna Chromophores for Luminescent Lanthanide Ions. *Chem. – Eur. J.* **4,** 2315–2323 (1998).

84. De Silva, C. R., Li, J., Zheng, Z. & Corrales, L. R. Correlation of Calculated Excited-state Energies and Experimental Quantum Yields of Luminescent Tb(III) β-diketonates. *J. Phys. Chem. A* **112,** 4527–4530 (2008).

85. He, P., Wang, H. H., Liu, S. G., Shi, J. X., Wang, G. & Gong, M. L. Visible-Light Excitable Europium(III) Complexes with 2,7-Positional Substituted Carbazole Group-Containing Ligands. *Inorg. Chem.* **48,** 11382–11387 (2009).

86. D'Aléo, A., Xu, J., Moore, E. G., Jocher, C. J. & Raymond, K. N. Aryl-Bridged 1-Hydroxypyridin-2-one: Sensitizer Ligands for Eu(III). *Inorg. Chem.* **47,** 6109–6111 (2008).

87. Divya, V., Freire, R. O. & Reddy, M. L. P. Tuning of the excitation wavelength from UV to visible region in Eu^{3+}-β-diketonate complexes: Comparison of theoretical and experimental photophysical properties. *Dalton Trans.* **40,** 3257–3268 (2011).

88. Divya, V., Biju, S., Varma, R. L. & Reddy, M. L. P. Highly efficient visible light sensitized red emission from europium tris[1-(4-biphenoyl)-3-(2-fluoroyl)propanedione](1,10-phenanthroline) complex grafted on silica nanoparticles. *J. Mater. Chem.* **20,** 5220–5227 (2010).

89. Divya, V. & Reddy, M. L. P. Visible-light excited red emitting luminescent nanocomposites derived from Eu^{3+} -phenathrene-based fluorinated β-diketonate complexes and multi-walled carbon nanotubes. *J Mater Chem C* **1,** 160–170 (2013).

90. De Sá, G. F., Malta, O. L., de Mello Donegá, C., Simas, A. M., Longo, R. L., Santa-Cruz, P. A. & da Silva Jr., E. F. Spectroscopic properties and design of highly luminescent lanthanide coordination complexes. *Coord. Chem. Rev.* **196,** 165–195 (2000).

91. Werts, M. H. V., Hofstraat, J. W., Geurts, F. A. J. & Verhoeven, J. W. Fluorescein and eosin as sensitizing chromophores in near-infrared luminescent ytterbium(III), neodymium(III) and erbium(III) chelates. *Chem. Phys. Lett.* **276,** 196–201 (1997).

92. Kleinerman, M. Energy Migration in Lanthanide Chelates. *J. Chem. Phys.* **51,** 2370–2381 (1969).

93. Yang, C., Fu, L.-M., Wang, Y., Zhang, J.-P., Wong, W.-T., Ai, X.-C., Qiao, Y.-F., Zou, B.-S. & Gui, L.-L. A Highly Luminescent Europium Complex Showing Visible-Light-Sensitized Red Emission: Direct Observation of the Singlet Pathway. *Angew. Chem. Int. Ed.* **43,** 5010–5013 (2004).

94. Fu, L.-M., Ai, X.-C., Li, M.-Y., Wen, X.-F., Hao, R., Wu, Y.-S., Wang, Y. & Zhang, J.-P. Role of Ligand-to-Metal Charge Transfer State in Nontriplet Photosensitization of Luminescent Europium Complex. *J. Phys. Chem. A* **114,** 4494–4500 (2010).

95. D'Aléo, A., Picot, A., Beeby, A., Gareth Williams, J. A., Le Guennic, B., Andraud, C. & Maury, O. Efficient Sensitization of Europium, Ytterbium, and Neodymium Functionalized Tris-Dipicolinate Lanthanide Complexes through Tunable Charge-Transfer Excited States. *Inorg. Chem.* **47,** 10258–10268 (2008).

96. Kim, Y. H., Baek, N. S. & Kim, H. K. Sensitized Emission of Luminescent Lanthanide Complexes Based on 4-Naphthalen-1-yl-Benzoic Acid Derivatives by a Charge-Transfer Process. *ChemPhysChem* **7,** 213–221 (2006).

97. H. V. Werts, M., A. Duin, M., W. Hofstraat, J. & W. Verhoeven, J. Bathochromicity of Michler's ketone upon coordination with lanthanide(III) [small beta]-diketonates enables efficient sensitisation of Eu3+ for luminescence under visible light excitation[dagger]. *Chem. Commun.* 799–800 (1999).

98. Puntus, L. N., Lyssenko, K. A., Antipin, M. Y. & Bünzli, J.-C. G. Role of Inner- and Outer-Sphere Bonding in the Sensitization of EuIII-Luminescence Deciphered by Combined Analysis of Experimental Electron Density Distribution Function and Photophysical Data. *Inorg. Chem.* **47,** 11095–11107 (2008).

99. Roh, S.-G., Baek, N.-S., Kim, Y.-H. & Kim, H.-K. Energy Transfer Pathway in Luminescent Lanthanide Complexes Based on Dansyl-N-methylaminobenzoic Acid through Intramolecular Charge Transfer State for Near Infrared Emission. *Bull. Korean Chem. Soc.* **28,** 1249–1255 (2007).

100. D'Aléo, A., Picot, A., Baldeck, P. L., Andraud, C. & Maury, O. Design of Dipicolinic Acid Ligands for the Two-Photon Sensitized Luminescence of Europium Complexes with Optimized Cross-Sections. *Inorg. Chem.* **47,** 10269–10279 (2008).

101. Puntus, L. N., Chauvin, A.-S., Varbanov, S. & Bünzli, J.-C. G. Lanthanide Complexes with a Calix[8]arene Bearing Phosphinoyl Pendant Arms. *Eur. J. Inorg. Chem.* **2007,** 2315–2326 (2007).

102. Kadjane, P., Charbonnière, L., Camerel, F., Lainé, P. P. & Ziessel, R. Improving visible light sensitization of luminescent europium complexes. *J. Fluoresc.* **18,** 119–129 (2008).

103. Shi, M., Ding, C., Dong, J., Wang, H., Tian, Y. & Hu, Z. A novel europium(III) complex with versatility in excitation ranging from infrared to ultraviolet. *Phys. Chem. Chem. Phys.* **11,** 5119–5123 (2009).

104. Puntus, L. N., Lyssenko, K. A., Pekareva, I. S. & Bünzli, J.-C. G. Intermolecular Interactions as

Actors in Energy-Transfer Processes in Lanthanide Complexes with 2,2′-Bipyridine. *J. Phys. Chem. B* **113,** 9265–9277 (2009).

105. Longo, R., Gonçalves e Silva, F. R. & Malta, O. L. A theoretical study of the energy-transfer process in $[Eu\subset bpy.bpy.bpy]^{3}+$ cryptates: a ligand-to-metal charge-transfer state? *Chem. Phys. Lett.* **328,** 67–74 (2000).

106. Gawryszewska, P., Malta, O. L., Longo, R. L., Goncalves e Silva, F. R., Alves, S., Mierzwicki, K., Latajka, Z., Pietraszkiewicz, M. & Legendziewicz, J. Experimental and Theoretical Study of the Photophysics and Structures of Europium Cryptates Incorporating 3,3'-Bi-isoquinoline-2,2'-dioxide. *ChemPhysChem* **5,** 1577–1584 (2004).

107. Carlos, L. D., Fernandes, J. A., Ferreira, R. A. S., Malta, O. L., Gonçalves, I. S. & Ribeiro-Claro, P. Emission quantum yield of a europium(III) tris-β-diketonate complex bearing a 1,4-diaza-1,3-butadiene: Comparison with theoretical prediction. *Chem. Phys. Lett.* **413,** 22–24 (2005).

108. Blasse, G. & Sabbatini, N. The quenching of rare-earth ion luminescence in molecular and non-molecular solids. *Mater. Chem. Phys.* **16,** 237–252 (1987).

109. Ward, M. D. Mechanisms of sensitization of lanthanide(III)-based luminescence in transition metal/lanthanide and anthracene/lanthanide dyads. *Coord. Chem. Rev.* **254,** 2634–2642 (2010).

110. Chen, F.-F., Chen, Z.-Q., Bian, Z.-Q. & Huang, C.-H. Sensitized luminescence from lanthanides in d–f bimetallic complexes. *Coord. Chem. Rev.* **254,** 991–1010 (2010).

111. Herrera, J.-M., Pope, S. J. A., Adams, H., Faulkner, S. & Ward, M. D. Structural and Photophysical Properties of Coordination Networks Combining [Ru(Bpym)(CN)4]2- or [{Ru(CN)4}2(μ-bpym)]4- Anions (bpym = 2,2'-Bipyrimidine) with Lanthanide(III) Cations: Sensitized Near-Infrared Luminescence from Yb(III), Nd(III), and Er(III) Following Ru-to-Lanthanide Energy Transfer. *Inorg. Chem.* **45,** 3895–3904 (2006).

112. Sénéchal-David, K., Pope, S. J. A., Quinn, S., Faulkner, S. & Gunnlaugsson, T. Sensitized Near-Infrared Lanthanide Luminescence from Nd(III)- and Yb(III)-Based Cyclen−Ruthenium Coordination Conjugates. *Inorg. Chem.* **45,** 10040–10042 (2006).

113. Baca, S. G., Adams, H., Sykes, D., Faulkner, S. & Ward, M. D. Three-component coordination networks based on $[Ru(phen)(CN)4]^{2-}$ anions, near-infrared luminescent lanthanide(iii) cations, and ancillary oligopyridine ligands: structures and photophysical properties. *Dalton Trans.* **23,** 2419–2430 (2007).

114. Pope, S. J. A., Coe, B. J., Faulkner, S., Bichenkova, E. V., Yu, X. & Douglas, K. T. Self-Assembly of Heterobimetallic d–f Hybrid Complexes: Sensitization of Lanthanide Luminescence by d-Block Metal-to-Ligand Charge-Transfer Excited States. *J. Am. Chem. Soc.* **126,** 9490–9491 (2004).

115. Shavaleev, N. M., Accorsi, G., Virgili, D., Bell, Z. R., Lazarides, T., Calogero, G., Armaroli, N. & Ward, M. D. Syntheses and Crystal Structures of Dinuclear Complexes Containing d-Block and f-Block Luminophores. Sensitization of NIR Luminescence from Yb(III), Nd(III), and Er(III) Centers by Energy Transfer from Re(I)− and Pt(II)−Bipyrimidine Metal Centers. *Inorg. Chem.* **44,** 61–72 (2005).

116. Kennedy, F., Shavaleev, N. M., Koullourou, T., Bell, Z. R., Jeffery, J. C., Faulkner, S. & Ward, M. D. Sensitised near-infrared luminescence from lanthanide(III) centres using Re(I) and Pt(II) diimine complexes as energy donors in d-f dinuclear complexes based on 2,3-bis(2-pyridyl)pyrazine. *Dalton Trans.* **15,** 1492–1499 (2007).

117. Pope, S. J. A., Coe, B. J. & Faulkner, S. Re(I) sensitised near-infrared lanthanide luminescence from a hetero-trinuclear Re_2Ln array. *Chem. Commun.* **13,** 1550–1551 (2004).

118. Sambrook, M. R., Curiel, D., Hayes, E. J., Beer, P. D., Pope, S. J. A. & Faulkner, S. Sensitised near infrared emission from lanthanides via anion-templated assembly of d-f heteronuclear [2]pseudorotaxanes. *New J. Chem.* **30,** 1133–1136 (2006).

119. Coppo, P., Duati, M., Kozhevnikov, V. N., Hofstraat, J. W. & De Cola, L. White-Light Emission from an Assembly Comprising Luminescent Iridium and Europium Complexes. *Angew. Chem. Int. Ed.* **44,** 1806–1810 (2005).

120. Sykes, D., Tidmarsh, I. S., Barbieri, A., Sazanovich, I. V., Weinstein, J. A. & Ward, M. D. d → f Energy Transfer in a Series of Ir^{III}/Eu^{III} Dyads: Energy-

Transfer Mechanisms and White-Light Emission. *Inorg. Chem.* **50,** 11323–11339 (2011).

121. Chen, F.-F., Bian, Z.-Q., Liu, Z.-W., Nie, D.-B., Chen, Z.-Q. & Huang, C.-H. Highly Efficient Sensitized Red Emission from Europium (III) in Ir–Eu Bimetallic Complexes by ^{3}MLCT Energy Transfer. *Inorg. Chem.* **47,** 2507–2513 (2008).

122. Li, X.-L., Dai, F.-R., Zhang, L.-Y., Zhu, Y.-M., Peng, Q. & Chen, Z.-N. Sensitization of Lanthanide Luminescence in Heterotrinuclear PtLn2 (Ln = Eu, Nd, Yb) Complexes with Terpyridyl-Functionalized Alkynyl by Energy Transfer from a Platinum(II) Alkynyl Chromophore. *Organometallics* **26,** 4483–4490 (2007).

123. Xu, H.-B., Shi, L.-X., Ma, E., Zhang, L.-Y., Wei, Q.-H. & Chen, Z.-N. Diplatinum alkynyl chromophores as sensitisers for lanthanide luminescence in Pt_2Ln_2 and Pt_2Ln_4 (Ln = Eu, Nd, Yb) arrays with acetylide-functionalized bipyridine/phenanthroline. *Chem. Commun.* **15,** 1601–1603 (2006).

124. Beeby, A., Bushby, L. M., Maffeo, D. & Williams, J. A. G. The efficient intramolecular sensitisation of terbium(III) and europium(III) by benzophenone-containing ligands. *J. Chem. Soc. Perkin Trans. 2* **7,** 1281–1283 (2000).

125. Bretonnière, Y., Cann, M. J., Parker, D. & Slater, R. Ratiometric probes for hydrogencarbonate analysis in intracellular or extracellular environments using europium luminescence. *Chem. Commun.* **17,** 1930–1931 (2002).

126. Dadabhoy, A., Faulkner, S. & Sammes, P. G. Small singlet–triplet energy gap of acridone enables longer wavelength sensitisation of europium(III) luminescence. *J. Chem. Soc. Perkin Trans. 2* **12,** 2359–2360 (2000).

127. Baggaley, E., Cao, D.-K., Sykes, D., Botchway, S. W., Weinstein, J. A. & Ward, M. D. Combined Two-Photon Excitation and d→f Energy Transfer in a Water-Soluble Ir^{III}/Eu^{III} Dyad: Two Luminescence Components from One Molecule for Cellular Imaging. *Chem. Weinh. Bergstr. Ger.* **20,** 8898–8903 (2014).

128. D'Aléo, A., Allali, M., Picot, A., Baldeck, P. L., Toupet, L., Andraud, C. & Maury, O. Sensitization of Eu(III) luminescence by donor-phenylethynyl-functionalized DTPA and DO3A macrocycles. *Comptes Rendus Chim.* **13,** 681–690 (2010).

129. Hemmilä, I., Mukkala, V.-M. & Takalo, H. Development of luminescent lanthanide chelate labels for diagnostic assays. *J. Alloys Compd.* **249,** 158–162 (1997).

130. Zhang, X.-F., Zhang, J. & Liu, L. Fluorescence Properties of Twenty Fluorescein Derivatives: Lifetime, Quantum Yield, Absorption and Emission Spectra. *J. Fluoresc.* **24,** 819–826 (2014).

131. Härmä, H., Soukka, T. & Lövgren, T. Europium Nanoparticles and Time-resolved Fluorescence for Ultrasensitive Detection of Prostate-specific Antigen. *Clin. Chem.* **47,** 561–568 (2001).

132. Kokko, L., Lövgren, T. & Soukka, T. Europium(III)-chelates embedded in nanoparticles are protected from interfering compounds present in assay media. *Anal. Chim. Acta* **585,** 17–23 (2007).

133. Haas, Y. & Stein, G. Pathways of radiative and radiationless transitions in europium(III) solutions. The role of high energy vibrations. *J. Phys. Chem.* **75,** 3677–3681 (1971).

134. Mathis, G. Rare earth cryptates and homogeneous fluoroimmunoassays with human sera. *Clin. Chem.* **39,** 1953–1959 (1993).

135. Wu, J., Ye, Z., Wang, G., Jin, D., Yuan, J., Guan, Y. & Piper, J. Visible-light-sensitized highly luminescent europium nanoparticles: preparation and application for time-gated luminescence bioimaging. *J. Mater. Chem.* **19,** 1258–1264 (2009).

136. Wu, Y., Shi, M., Zhao, L., Feng, W., Li, F. & Huang, C. Visible-light-excited and europium-emissive nanoparticles for highly-luminescent bioimaging in vivo. *Biomaterials* **35,** 5830–5839 (2014).

137. Wen, X., Li, M., Wang, Y., Zhang, J., Fu, L., Hao, R., Ma, Y. & Ai, X. Colloidal Nanoparticles of a Europium Complex with Enhanced Luminescent Properties. *Langmuir* **24,** 6932–6936 (2008).

138. Xue, F.-M., Liang, M.-H., Wang, Z.-H., Luan, L.-Y., Li, F.-W., Cheng, Y. & Shao, G.-S. The preparation and performance of visible-light-sensitized luminescent nanoparticles based on europium complex. *Chin. Chem. Lett.* **25,** 247–252 (2014).

139. Zhang, L., Tian, L., Ye, Z., Song, B. & Yuan, J. Preparation of visible-light-excited europium biolabels for time-resolved luminescence cell imaging application. *Talanta* **108,** 143–149 (2013).

140. Blomberg, K. R., Mukkala, V.-M., Hakala, H. H. O., Mäkinen, P. H., Suonpää, M. U. & Hemmilä, I. A. A dissociative fluorescence enhancement technique for one-step time-resolved immunoassays. *Anal. Bioanal. Chem.* **399,** 1677–1682 (2011).

141. Life Sciences Citation Library. *Life Sci. Cit. Libr.* at <http://citations.perkinelmer.com/>

142. Von Lode, P., Rosenberg, J., Pettersson, K. & Takalo, H. A Europium Chelate for Quantitative Point-of-Care Immunoassays Using Direct Surface Measurement. *Anal. Chem.* **75,** 3193–3201 (2003).

143. Takalo, H., Mukkala, V.-M., Mikola, H., Liitti, P. & Hemmilä, I. Synthesis of Europium(III) Chelates Suitable for Labeling of Bioactive Molecules. *Bioconjug. Chem.* **5,** 278–282 (1994).

144. Mukkala, V.-M. & Kankare, J. J. New 2,2′-Bipyridine Derivatives and Their Luminescence Properties with Europium(III) and Terbium(III) Ions. *Helv. Chim. Acta* **75,** 1578–1592 (1992).

145. Mukkala, V.-M., Sund, C., Kwiatkowski, M., Pasanen, P., Högberg, M., Kankare, J. & Takalo, H. New Heteroaromatic Complexing Agents and Luminescence of Their Europium(III) and Terbium(III) Chelates. *Helv. Chim. Acta* **75,** 1621–1632 (1992).

146. Mukkala, V.-M., Kwiatkowski, M., Kankare, J. & Takalo, H. Influence of Chelating Groups on the Luminescence Properties of Europium(III) and Terbium(III) chelates in the 2,2′-bipyridine series. *Helv. Chim. Acta* **76,** 893–899 (1993).

147. Takalo, H., Hänninen, E. & Kankare, J. Luminescence of Europium(III) Chelates with 4-(Arylethynyl)pyridines as Ligands. *Helv. Chim. Acta* **76,** 877–883 (1993).

148. Ylikotila, J., Välimaa, L., Vehniäinen, M., Takalo, H., Lövgren, T. & Pettersson, K. A sensitive TSH assay in spot-coated microwells utilizing recombinant antibody fragments. *J. Immunol. Methods* **306,** 104–114 (2005).

149. Nurmi, J., Ylikoski, A., Soukka, T., Karp, M. & Lövgren, T. A new label technology for the detection of specific polymerase chain reaction products in a closed tube. *Nucleic Acids Res.* **28,** e28–00 (2000).

150. Kokko, T., Kokko, L., Soukka, T. & Lövgren, T. Homogeneous non-competitive bioaffinity assay based on fluorescence resonance energy transfer. *Anal. Chim. Acta* **585,** 120–125 (2007).

151. Oser, A. & Valet, G. Nonradioactive Assay of DNA Hybridization by DNA-Template-Mediated Formation of a Ternary TbIII Complex in Pure Liquid Phase. *Angew. Chem. Int. Ed. Engl.* **29,** 1167–1169 (1990).

152. Wang, X., Chang, H., Xie, J., Zhao, B., Liu, B., Xu, S., Pei, W., Ren, N., Huang, L. & Huang, W. Recent developments in lanthanide-based luminescent probes. *Coord. Chem. Rev.* **273–274,** 201–212 (2014).

153. Sidelmann, J. J., Gram, J., Larsen, A., Overgaard, K. & Jespersen, J. Analytical and clinical validation of a new point-of-care testing system for determination of D-Dimer in human blood. *Thromb. Res.* **126,** 524–530 (2010).

154. Pettersson, K. & Lövgren, T. One-step all-in-one dry reagent immunoassay. US6429026 (B1) (1996).

155. Hagren, V., Lode, P. von, Syrjälä, A., Soukka, T., Lövgren, T., Kojola, H. & Nurmi, J. An automated PCR platform with homogeneous time-resolved fluorescence detection and dry chemistry assay kits. *Anal. Biochem.* **374,** 411–416 (2008).

156. Lode, P. von, Syrjälä, A., Hagren, V., Kojola, H., Soukka, T., Lövgren, T. & Nurmi, J. Fully Automated, Homogeneous Nucleic Acid Detection Technology Based on Dry-Reagent Assay Chemistry and Time-Resolved Fluorometry. *Clin. Chem.* **53,** 2014–2017 (2007).

157. Hirvonen, J. J., Nevalainen, M., Tissari, P., Salmenlinna, S., Rantakokko-Jalava, K. & Kaukoranta, S.-S. Rapid confirmation of suspected methicillin-resistant Staphylococcus aureus colonies on chromogenic agars by a new commercial PCR assay, the GenomEra MRSA/SA Diagnose. *Eur. J. Clin. Microbiol. Infect. Dis. Off. Publ. Eur. Soc. Clin. Microbiol.* **31,** 1961–1968 (2012).

158. Lehmusvuori, A., Juntunen, E., Tapio, A.-H., Rantakokko-Jalava, K., Soukka, T. & Lövgren, T. Rapid homogeneous PCR assay for the detection of Chlamydia trachomatis in urine samples. *J. Microbiol. Methods* **83,** 302–306 (2010).

159. Song, X. & Knotts, M. Time-resolved luminescent lateral flow assay technology. *Anal. Chim. Acta* **626,** 186–192 (2008).

160. Pettersson, K., von Lode, P., Eriksson, S., Lövgren, J. & Takalo, H. Multi-Assay Point-of-Care Platform: Highly Sensitive Time-Resolved Fluorometric Detection in Combination with a Universal 'All-In-One' Assay Format. *J. -Patient Test.* **2,** 225–232 (2003).

161. Lode, P. von, Rainaho, J. & Pettersson, K. Quantitative, Wide-Range, 5-Minute Point-of-Care Immunoassay for Total Human Chorionic Gonadotropin in Whole Blood. *Clin. Chem.* **50,** 1026–1035 (2004).

162. Pelkkikangas, A.-M., Jaakohuhta, S., Lövgren, T. & Härmä, H. Simple, rapid, and sensitive thyroid-stimulating hormone immunoassay using europium(III) nanoparticle label. *Anal. Chim. Acta* **517,** 169–176 (2004).

163. Von Lode, P., Hagrén, V., Palenius, T. & Lövgren, T. One-step quantitative thyrotropin assay for the detection of hypothyroidism in point-of-care conditions. *Clin. Biochem.* **36,** 121–128 (2003).

164. Päkkilä, H., Malmi, E., Lahtinen, S. & Soukka, T. Rapid homogeneous immunoassay for cardiac troponin I using switchable lanthanide luminescence. *Biosens. Bioelectron.* **62,** 201–207 (2014).

165. Hyytiä, H., Järvenpää, M.-L., Ristiniemi, N., Lövgren, T. & Pettersson, K. A comparison of capture antibody fragments in cardiac troponin I immunoassay. *Clin. Biochem.* **46,** 963–968 (2013).

166. Borisov, S. M. & Wolfbeis, O. S. Temperature-Sensitive Europium(III) Probes and Their Use for Simultaneous Luminescent Sensing of Temperature and Oxygen. *Anal. Chem.* **78,** 5094–5101 (2006).

167. Borisov, S. M. & Klimant, I. Blue LED excitable temperature sensors based on a new europium(III) chelate. *J. Fluoresc.* **18,** 581–589 (2008).

168. Jin, D., Connally, R. & Piper, J. Practical time-gated luminescence flow cytometry. II: Experimental evaluation using UV LED excitation. *Cytometry A* **71A,** 797–808 (2007).

169. Connally, R., Jin, D. & Piper, J. High intensity solid-state UV source for time-gated luminescence microscopy. *Cytometry A* **69A,** 1020–1027 (2006).

170. Leif, R. C., Vallarino, L. M., Becker, M. C. & Yang, S. Increasing lanthanide luminescence by use of the RETEL effect. *Cytometry A* **69A,** 940–946 (2006).

171. Gahlaut, N. & Miller, L. W. Time-resolved microscopy for imaging lanthanide luminescence in living cells. *Cytom. Part J. Int. Soc. Anal. Cytol.* **77,** 1113–1125 (2010).

172. Connally, R., Veal, D. & Piper, J. Time-resolved fluorescence microscopy using an improved europium chelate BHHST for the in situ detection of Cryptosporidium and Giardia. *Microsc. Res. Tech.* **64,** 312–322 (2004).

173. Li, X., Zhang, F. & Zhao, D. Highly efficient lanthanide upconverting nanomaterials: Progresses and challenges. *Nano Today* **8,** 643–676 (2013).

174. He, G. S., Tan, L.-S., Zheng, Q. & Prasad, P. N. Multiphoton Absorbing Materials: Molecular Designs, Characterizations, and Applications. *Chem. Rev.* **108,** 1245–1330 (2008).

175. Zhao, J., Ji, S. & Guo, H. Triplet–triplet annihilation based upconversion: from triplet sensitizers and triplet acceptors to upconversion quantum yields. *RSC Adv.* **1,** 937–950 (2011).

176. Dong, H., Sun, L.-D. & Yan, C.-H. Energy transfer in lanthanide upconversion studies for extended optical applications. *Chem Soc Rev* (2015). doi:10.1039/C4CS00188E

177. Ma, Y. & Wang, Y. Recent advances in the sensitized luminescence of organic europium complexes. *Coord. Chem. Rev.* **254,** 972–990 (2010).

178. Nattestad, A., Cheng, Y. Y., MacQueen, R. W., Schulze, T. F., Thompson, F. W., Mozer, A. J., Fückel, B., Khoury, T., Crossley, M. J., Lips, K., Wallace, G. G. & Schmidt, T. W. Dye-Sensitized Solar Cell with Integrated Triplet–Triplet Annihilation Upconversion System. *J. Phys. Chem. Lett.* **4,** 2073–2078 (2013).

179. Wang, F. & Liu, X. Recent advances in the chemistry of lanthanide-doped upconversion nanocrystals. *Chem. Soc. Rev.* **38,** 976–989 (2009).

180. Vuojola, J., Riuttamäki, T., Kulta, E., Arppe, R. & Soukka, T. Fluorescence-quenching-based homogeneous caspase-3 activity assay using photon upconversion. *Anal. Chim. Acta* **725,** 67–73 (2012).

181. Kale, V., Lastusaari, M., Hölsä, J. & Soukka, T. Intense UV upconversion through highly sensitized $NaRF_4$:Tm (R:Y,Yb) crystals. *RSC Adv.* **5,** 35858–35865 (2015).

182. Strohhöfer, C. & Polman, A. Absorption and emission spectroscopy in Er^{3+}–Yb^{3+} doped aluminum oxide waveguides. *Opt. Mater.* **21,** 705–712 (2003).

183. Wang, J., Deng, R., MacDonald, M. A., Chen, B., Yuan, J., Wang, F., Chi, D., Andy Hor, T. S., Zhang, P., Liu, G., Han, Y. & Liu, X. Enhancing multiphoton upconversion through energy clustering at sublattice level. *Nat. Mater.* **13,** 157–162 (2014).

184. Auzel, F. Upconversion and Anti-Stokes Processes with f and d Ions in Solids. *Chem. Rev.* **104,** 139–174 (2004).

185. Sun, L.-D., Dong, H., Zhang, P.-Z. & Yan, C.-H. Upconversion of Rare Earth Nanomaterials. *Annu. Rev. Phys. Chem.* **66,** 619–642 (2015).

186. Wang, Y.-F., Liu, G.-Y., Sun, L.-D., Xiao, J.-W., Zhou, J.-C. & Yan, C.-H. Nd3+-Sensitized Upconversion Nanophosphors: Efficient In Vivo Bioimaging Probes with Minimized Heating Effect. *ACS Nano* **7,** 7200–7206 (2013).

187. Xie, X., Gao, N., Deng, R., Sun, Q., Xu, Q.-H. & Liu, X. Mechanistic Investigation of Photon Upconversion in Nd^{3+}-Sensitized Core–Shell Nanoparticles. *J. Am. Chem. Soc.* **135,** 12608–12611 (2013).

188. Shen, J., Chen, G., Ohulchanskyy, T. Y., Kesseli, S. J., Buchholz, S., Li, Z., Prasad, P. N. & Han, G. Tunable Near Infrared to Ultraviolet Upconversion Luminescence Enhancement in (α-$NaYF_4$:Yb,Tm)/CaF_2 Core/Shell Nanoparticles for In situ Real-time Recorded Biocompatible Photoactivation. *Small* **9,** 3213–3217 (2013).

189. Wen, H., Zhu, H., Chen, X., Hung, T. F., Wang, B., Zhu, G., Yu, S. F. & Wang, F. Upconverting Near-Infrared Light through Energy Management in Core-Shell-Shell Nanoparticles. *Angew. Chem.* **125,** 13661–13665 (2013).

190. Suyver, J. F., Grimm, J., van Veen, M. K., Biner, D., Krämer, K. W. & Güdel, H. U. Upconversion spectroscopy and properties of $NaYF_4$ doped with Er^{3+}, Tm^{3+} and/or Yb^{3+}. *J. Lumin.* **117,** 1–12 (2006).

191. Yi, G. S. & Chow, G. M. Synthesis of Hexagonal-Phase $NaYF_4$:Yb,Er and $NaYF_4$:Yb,Tm Nanocrystals with Efficient Up-Conversion Fluorescence. *Adv. Funct. Mater.* **16,** 2324–2329 (2006).

192. Liu, G. Advances in the theoretical understanding of photon upconversion in rare-earth activated nanophosphors. *Chem Soc Rev* (2015). doi:10.1039/C4CS00187G

193. Longmire, M., Choyke, P. L. & Kobayashi, H. Clearance properties of nano-sized particles and molecules as imaging agents: considerations and caveats. *Nanomed.* **3,** 703–717 (2008).

194. Gargas, D. J., Chan, E. M., Ostrowski, A. D., Aloni, S., Altoe, M. V. P., Barnard, E. S., Sanii, B., Urban, J. J., Milliron, D. J., Cohen, B. E. & Schuck, P. J. Engineering bright sub-10-nm upconverting nanocrystals for single-molecule imaging. *Nat. Nanotechnol.* **9,** 300–305 (2014).

195. Wang, F., Wang, J. & Liu, X. Direct Evidence of a Surface Quenching Effect on Size-Dependent Luminescence of Upconversion Nanoparticles. *Angew. Chem. Int. Ed.* **49,** 7456–7460 (2010).

196. Ostrowski, A. D., Chan, E. M., Gargas, D. J., Katz, E. M., Han, G., Schuck, P. J., Milliron, D. J. & Cohen, B. E. Controlled Synthesis and Single-Particle Imaging of Bright, Sub-10 nm Lanthanide-Doped Upconverting Nanocrystals. *ACS Nano* **6,** 2686–2692 (2012).

197. Zhao, J., Lu, Z., Yin, Y., McRae, C., Piper, J. A., Dawes, J. M., Jin, D. & Goldys, E. M. Upconversion luminescence with tunable lifetime in $NaYF_4$:Yb,Er nanocrystals: role of nanocrystal size. *Nanoscale* **5,** 944–952 (2013).

198. Boyer, J.-C. & van Veggel, F. C. J. M. Absolute quantum yield measurements of colloidal $NaYF_4$: Er^{3+}, Yb^{3+} upconverting nanoparticles. *Nanoscale* **2,** 1417–1419 (2010).

199. Yang, T., Sun, Y., Liu, Q., Feng, W., Yang, P. & Li, F. Cubic sub-20 nm $NaLuF_4$-based upconversion nanophosphors for high-contrast bioimaging in different animal species. *Biomaterials* **33,** 3733–3742 (2012).

200. Yi, G.-S. & Chow, G.-M. Water-Soluble $NaYF_4$:Yb,Er(Tm)/$NaYF_4$/Polymer Core/Shell/Shell Nanoparticles with Significant Enhancement of Upconversion Fluorescence. *Chem. Mater.* **19,** 341–343 (2007).

201. Vetrone, F., Naccache, R., Mahalingam, V., Morgan, C. G. & Capobianco, J. A. The Active-Core/Active-Shell Approach: A Strategy to Enhance the Upconversion Luminescence in

Lanthanide-Doped Nanoparticles. *Adv. Funct. Mater.* **19,** 2924–2929 (2009).

202. Chen, X., Peng, D., Ju, Q. & Wang, F. Photon upconversion in core–shell nanoparticles. *Chem Soc Rev* **44,** 1318–1330 (2015).

203. Yuan, D., Tan, M. C., Riman, R. E. & Chow, G. M. Comprehensive Study on the Size Effects of the Optical Properties of NaYF4:Yb,Er Nanocrystals. *J. Phys. Chem. C* **117,** 13297–13304 (2013).

204. Zou, W., Visser, C., Maduro, J. A., Pshenichnikov, M. S. & Hummelen, J. C. Broadband dye-sensitized upconversion of near-infrared light. *Nat. Photonics* **6,** 560–564 (2012).

205. Wu, D. M., García-Etxarri, A., Salleo, A. & Dionne, J. A. Plasmon-Enhanced Upconversion. *J. Phys. Chem. Lett.* **5,** 4020–4031 (2014).

206. Sedlmeier, A. & Gorris, H. H. Surface modification and characterization of photon-upconverting nanoparticles for bioanalytical applications. *Chem Soc Rev* **44,** 1526–1560 (2015).

207. Haase, M. & Schäfer, H. Upconverting nanoparticles. *Angew. Chem.* **50,** 5808–29 (2011).

208. Lin, M., Zhao, Y., Wang, S., Liu, M., Duan, Z., Chen, Y., Li, F., Xu, F. & Lu, T. Recent advances in synthesis and surface modification of lanthanide-doped upconversion nanoparticles for biomedical applications. *Biotechnol. Adv.* **30,** 1551–1561 (2012).

209. Boyer, J.-C., Vetrone, F., Cuccia, L. A. & Capobianco, J. A. Synthesis of Colloidal Upconverting NaYF4 Nanocrystals Doped with Er3+, Yb3+ and Tm3+, Yb3+ via Thermal Decomposition of Lanthanide Trifluoroacetate Precursors. *J. Am. Chem. Soc.* **128,** 7444–7445 (2006).

210. König, K. Multiphoton microscopy in life sciences. *J. Microsc.* **200,** 83–104 (2000).

211. Song, Z., Anissimov, Y. G., Zhao, J., Nechaev, A. V., Nadort, A., Jin, D., Prow, T. W., Roberts, M. S. & Zvyagin, A. V. Background free imaging of upconversion nanoparticle distribution in human skin. *J. Biomed. Opt.* **18,** 061215–061215 (2012).

212. Wu, S., Han, G., Milliron, D. J., Aloni, S., Altoe, V., Talapin, D. V., Cohen, B. E. & Schuck, P. J. Non-blinking and photostable upconverted luminescence from single lanthanide-doped nanocrystals. *Proc. Natl. Acad. Sci.* **106,** 10917–10921 (2009).

213. Wright, W. H., Mufti, N. A., Tagg, N. T., Webb, R. R. & Schneider, L. V. High-sensitivity immunoassay using a novel upconverting phosphor reporter. in **2985,** 248–255 (1997).

214. Zijlmans, H. J. M. A. A., Bonnet, J., Burton, J., Kardos, K., Vail, T., Niedbala, R. S. & Tanke, H. J. Detection of Cell and Tissue Surface Antigens Using Up-Converting Phosphors: A New Reporter Technology. *Anal. Biochem.* **267,** 30–36 (1999).

215. Van de Rijke, F., Zijlmans, H., Li, S., Vail, T., Raap, A. K., Niedbala, R. S. & Tanke, H. J. Up-converting phosphor reporters for nucleic acid microarrays. *Nat. Biotechnol.* **19,** 273–276 (2001).

216. Lu, H., Yi, G., Zhao, S., Chen, D., Guo, L.-H. & Cheng, J. Synthesis and characterization of multi-functional nanoparticles possessing magnetic, up-conversion fluorescence and bio-affinity properties. *J. Mater. Chem.* **14,** 1336 (2004).

217. Päkkilä, H., Ylihärsilä, M., Lahtinen, S., Hattara, L., Salminen, N., Arppe, R., Lastusaari, M., Saviranta, P. & Soukka, T. Quantitative Multianalyte Microarray Immunoassay Utilizing Upconverting Phosphor Technology. *Anal. Chem.* **84,** 8628–8634 (2012).

218. Ylihärsilä, M., Harju, E., Arppe, R., Hattara, L., Hölsä, J., Saviranta, P., Soukka, T. & Waris, M. Genotyping of clinically relevant human adenoviruses by array-in-well hybridization assay. *Clin. Microbiol. Infect.* **19,** 551–557 (2013).

219. Wang, L., Yan, R., Huo, Z., Wang, L., Zeng, J., Bao, J., Wang, X., Peng, Q. & Li, Y. Fluorescence Resonant Energy Transfer Biosensor Based on Upconversion-Luminescent Nanoparticles. *Angew. Chem. Int. Ed.* **44,** 6054–6057 (2005).

220. Kuningas, K., Rantanen, T., Ukonaho, T., Lövgren, T. & Soukka, T. Homogeneous Assay Technology Based on Upconverting Phosphors. *Anal. Chem.* **77,** 7348–7355 (2005).

221. Kuningas, K., Ukonaho, T., Päkkilä, H., Rantanen, T., Rosenberg, J., Lövgren, T. & Soukka, T. Upconversion Fluorescence Resonance Energy Transfer in a Homogeneous Immunoassay for Estradiol. *Anal. Chem.* **78,** 4690–4696 (2006).

222. Kuningas, K., Päkkilä, H., Ukonaho, T., Rantanen, T., Lövgren, T. & Soukka, T. Upconversion

Fluorescence Enables Homogeneous Immunoassay in Whole Blood. *Clin. Chem.* **53,** 145–146 (2007).

223. Jiang, S. & Zhang, Y. Upconversion Nanoparticle-Based FRET System for Study of siRNA in Live Cells. *Langmuir* **26,** 6689–6694 (2010).

224. Rantanen, T., Järvenpää, M.-L., Vuojola, J., Arppe, R., Kuningas, K. & Soukka, T. Upconverting phosphors in a dual-parameter LRET-based hybridization assay. *Analyst* **134,** 1713–1716 (2009).

225. Wang, Y., Bao, L., Liu, Z. & Pang, D.-W. Aptamer Biosensor Based on Fluorescence Resonance Energy Transfer from Upconverting Phosphors to Carbon Nanoparticles for Thrombin Detection in Human Plasma. *Anal. Chem.* **83,** 8130–8137 (2011).

226. Zhang, C., Yuan, Y., Zhang, S., Wang, Y. & Liu, Z. Biosensing Platform Based on Fluorescence Resonance Energy Transfer from Upconverting Nanocrystals to Graphene Oxide. *Angew. Chem. Int. Ed.* **50,** 6851–6854 (2011).

227. Mattsson, L., Wegner, K. D., Hildebrandt, N. & Soukka, T. Upconverting nanoparticle to quantum dot FRET for homogeneous double-nano biosensors. *RSC Adv.* **5,** 13270–13277 (2015).

228. Sun, L.-N., Peng, H., Stich, M. I. J., Achatz, D. & Wolfbeis, O. S. pH sensor based on upconverting luminescent lanthanide nanorods. *Chem. Commun.* **33,** 5000–5002 (2009).

229. Ali, R., Saleh, S. M., Meier, R. J., Azab, H. A., Abdelgawad, I. I. & Wolfbeis, O. S. Upconverting nanoparticle based optical sensor for carbon dioxide. *Sens. Actuators B Chem.* **150,** 126–131 (2010).

230. Mader, H. S. & Wolfbeis, O. S. Optical Ammonia Sensor Based on Upconverting Luminescent Nanoparticles. *Anal. Chem.* **82,** 5002–5004 (2010).

231. Liu, Q., Peng, J., Sun, L. & Li, F. High-Efficiency Upconversion Luminescent Sensing and Bioimaging of Hg(II) by Chromophoric Ruthenium Complex-Assembled Nanophosphors. *ACS Nano* **5,** 8040–8048 (2011).

232. Liu, J., Liu, Y., Liu, Q., Li, C., Sun, L. & Li, F. Iridium(III) Complex-Coated Nanosystem for Ratiometric Upconversion Luminescence Bioimaging of Cyanide Anions. *J. Am. Chem. Soc.* **133,** 15276–15279 (2011).

233. Vetrone, F., Naccache, R., Zamarrón, A., Juarranz de la Fuente, A., Sanz-Rodríguez, F., Martinez Maestro, L., Martín Rodriguez, E., Jaque, D., García Solé, J. & Capobianco, J. A. Temperature Sensing Using Fluorescent Nanothermometers. *ACS Nano* **4,** 3254–3258 (2010).

234. Liu, B., Tan, H. & Chen, Y. Upconversion nanoparticle-based fluorescence resonance energy transfer assay for Cr(III) ions in urine. *Anal. Chim. Acta* **761,** 178–185 (2013).

235. Wilhelm, S., del Barrio, M., Heiland, J., Himmelstoß, S. F., Galbán, J., Wolfbeis, O. S. & Hirsch, T. Spectrally Matched Upconverting Luminescent Nanoparticles for Monitoring Enzymatic Reactions. *ACS Appl. Mater. Interfaces* **6,** 15427–15433 (2014).

236. Harvey, P., Oakland, C., Driscoll, M. D., Hay, S. & Natrajan, L. S. Ratiometric detection of enzyme turnover and flavin reduction using rare-earth upconverting phosphors. *Dalton Trans.* **43,** 5265 (2014).

237. Bosschaart, N., Edelman, G. J., Aalders, M. C. G., van Leeuwen, T. G. & Faber, D. J. A literature review and novel theoretical approach on the optical properties of whole blood. *Lasers Med. Sci.* **29,** 453–479 (2014).

238. Hönes, J., Müller, P. & Surridge, N. The Technology Behind Glucose Meters: Test Strips. *Diabetes Technol. Ther.* **10,** S–10 (2008).

239. Wang, H.-C. & Lee, A.-R. Recent developments in blood glucose sensors. *J. Food Drug Anal.* (2015). doi:10.1016/j.jfda.2014.12.001

240. Ballerstadt, R., Evans, C., McNichols, R. & Gowda, A. Concanavalin A for in vivo glucose sensing: A biotoxicity review. *Biosens. Bioelectron.* **22,** 275–284 (2006).

241. Hansen, J. S., Christensen, J. B., Petersen, J. F., Hoeg-Jensen, T. & Norrild, J. C. Arylboronic acids: A diabetic eye on glucose sensing. *Sens. Actuators B Chem.* **161,** 45–79 (2012).

242. Peng, J., Wang, Y., Wang, J., Zhou, X. & Liu, Z. A new biosensor for glucose determination in serum based on up-converting fluorescence resonance energy transfer. *Biosens. Bioelectron.* **28,** 414–420 (2011).

243. Del Barrio, M., de Marcos, S., Cebolla, V., Heiland, J., Wilhelm, S., Hirsch, T. & Galbán, J. Enzyme-

induced modulation of the emission of upconverting nanoparticles: Towards a new sensing scheme for glucose. *Biosens. Bioelectron.* **59,** 14–20 (2014).

244. He, M. & Liu, Z. Paper-Based Microfluidic Device with Upconversion Fluorescence Assay. *Anal. Chem.* **85,** 11691–11694 (2013).

245. Van Dam, G. J., de Dood, C. J., Lewis, M., Deelder, A. M., van Lieshout, L., Tanke, H. J., van Rooyen, L. H. & Corstjens, P. L. A. M. A robust dry reagent lateral flow assay for diagnosis of active schistosomiasis by detection of Schistosoma circulating anodic antigen. *Exp. Parasitol.* **135,** 274–282 (2013).

246. Corstjens, P. L. A. M., Lieshout, L. van, Zuiderwijk, M., Kornelis, D., Tanke, H. J., Deelder, A. M. & Dam, G. J. van. Up-Converting Phosphor Technology-Based Lateral Flow Assay for Detection of Schistosoma Circulating Anodic Antigen in Serum. *J. Clin. Microbiol.* **46,** 171–176 (2008).

247. Li, L., Zhou, L., Yu, Y., Zhu, Z., Lin, C., Lu, C. & Yang, R. Development of up-converting phosphor technology-based lateral-flow assay for rapidly quantitative detection of hepatitis B surface antibody. *Diagn. Microbiol. Infect. Dis.* **63,** 165–172 (2009).

248. Bobosha, K., Tjon Kon Fat, E. M., van den Eeden, S. J. F., Bekele, Y., van der Ploeg-van Schip, J. J., de Dood, C. J., Dijkman, K., Franken, K. L. M. C., Wilson, L., Aseffa, A., Spencer, J. S., Ottenhoff, T. H. M., Corstjens, P. L. A. M. & Geluk, A. Field-Evaluation of a New Lateral Flow Assay for Detection of Cellular and Humoral Immunity against Mycobacterium leprae. *PLoS Negl. Trop. Dis.* **8,** (2014).

249. Corstjens, P. L. A. M., Fidder, H. H., Wiesmeijer, K. C., de Dood, C. J., Rispens, T., Wolbink, G.-J., Hommes, D. W. & Tanke, H. J. A rapid assay for on-site monitoring of infliximab trough levels: a feasibility study. *Anal. Bioanal. Chem.* **405,** 7367–7375 (2013).

250. Chen, Z., Abrams, W. R., Geva, E., de Dood, C. J., Gonz&#xe1, Lez, J., M, S., Tanke, H. J., Niedbala, R. S., Zhou, P., Malamud, D. & Corstjens, P. L. A. M. Development of a Generic Microfluidic Device for Simultaneous Detection of Antibodies and Nucleic Acids in Oral Fluids. *BioMed Res. Int.* **2013,** e543294 (2013).

251. Zhao, P., Wu, Y., Zhu, Y., Yang, X., Jiang, X., Xiao, J., Zhang, Y. & Li, C. Upconversion fluorescent strip sensor for rapid determination of Vibrio anguillarum. *Nanoscale* **6,** 3804–3809 (2014).

252. Yan, Z., Zhou, L., Zhao, Y., Wang, J., Huang, L., Hu, K., Liu, H., Wang, H., Guo, Z., Song, Y., Huang, H. & Yang, R. Rapid quantitative detection of Yersinia pestis by lateral-flow immunoassay and up-converting phosphor technology-based biosensor. *Sens. Actuators B Chem.* **119,** 656–663 (2006).

253. Niedbala, R. S., Feindt, H., Kardos, K., Vail, T., Burton, J., Bielska, B., Li, S., Milunic, D., Bourdelle, P. & Vallejo, R. Detection of analytes by immunoassay using up-converting phosphor technology. *Anal. Biochem.* **293,** 22–30 (2001).

254. Corstjens, P. L. a. M., Chen, Z., Zuiderwijk, M., Bau, H. H., Abrams, W. R., Malamud, D., Sam Niedbala, R. & Tanke, H. J. Rapid Assay Format for Multiplex Detection of Humoral Immune Responses to Infectious Disease Pathogens (HIV, HCV, and TB). *Ann. N. Y. Acad. Sci.* **1098,** 437–445 (2007).

255. Corstjens, P. L. A. M., Zuiderwijk, M., Tanke, H. J., van der Ploeg-van Schip, J. J., Ottenhoff, T. H. M. & Geluk, A. A user-friendly, highly sensitive assay to detect the IFN-γ secretion by T cells. *Clin. Biochem.* **41,** 440–444 (2008).

256. Corstjens, P. L. A. M., de Dood, C. J., van der Ploeg-van Schip, J. J., Wiesmeijer, K. C., Riuttamäki, T., van Meijgaarden, K. E., Spencer, J. S., Tanke, H. J., Ottenhoff, T. H. M. & Geluk, A. Lateral flow assay for simultaneous detection of cellular- and humoral immune responses. *Clin. Biochem.* **44,** 1241–1246 (2011).

257. Wang, J., Chen, Z., Corstjens, P. L. A. M., Mauk, M. G. & Bau, H. H. A disposable microfluidic cassette for DNA amplification and detection. *Lab Chip* **6,** 46–53 (2006).

258. Chen, Z., Mauk, M. G., Wang, J., Abrams, W. R., Corstjens, P. L. a. M., Niedbala, R. S., Malamud, D. & Bau, H. H. A Microfluidic System for Saliva-Based Detection of Infectious Diseases. *Ann. N. Y. Acad. Sci.* **1098,** 429–436 (2007).

259. Abrams, W. R., Barber, C. A., Mccann, K., Tong, G., Chen, Z., Mauk, M. G., Wang, J., Volkov, A., Bourdelle, P., Corstjens, P. L. A. M., Zuiderwijk, M., Kardos, K., Li, S., Tanke, H. J., Sam Niedbala, R., Malamud, D. & Bau, H. Development of a Microfluidic Device for Detection of Pathogens in Oral Samples Using Upconverting Phosphor Technology (UPT). *Ann. N. Y. Acad. Sci.* **1098,** 375–388 (2007).

260. Chen, D., Mauk, M., Qiu, X., Liu, C., Kim, J., Ramprasad, S., Ongagna, S., Abrams, W. R., Malamud, D., Corstjens, P. L. A. M. & Bau, H. H. An integrated, self-contained microfluidic cassette for isolation, amplification, and detection of nucleic acids. *Biomed. Microdevices* **12,** 705–719 (2010).

261. Ongagna-Yhombi, S. Y., Corstjens, P., Geva, E., Abrams, W. R., Barber, C. A., Malamud, D. & Mharakurwa, S. Improved assay to detect Plasmodium falciparum using an uninterrupted, semi-nested PCR and quantitative lateral flow analysis. *Malar. J.* **12,** 74–81 (2013).

262. Malamud, D., Bau, H., Niedbala, S. & Corstjens, P. Point Detection of Pathogens in Oral Samples. *Adv. Dent. Res.* **18,** 12–16 (2005).

263. Qiu, X., Thompson, J. A., Chen, Z., Liu, C., Chen, D., Ramprasad, S., Mauk, M. G., Ongagna, S., Barber, C., Abrams, W. R., Malamud, D., Corstjens, P. L. A. M. & Bau, H. H. Finger-actuated, self-contained immunoassay cassettes. *Biomed. Microdevices* **11,** 1175–1186 (2009).

264. Liu, C., Qiu, X., Ongagna, S., Chen, D., Chen, Z., Abrams, W. R., Malamud, D., Corstjens, P. L. A. M. & Bau, H. H. A timer-actuated immunoassay cassette for detecting molecular markers in oral fluids. *Lab Chip* **9,** 768–776 (2009).

265. Hampl, J., Hall, M., Mufti, N. A., Yao, Y. M., MacQueen, D. B., Wright, W. H. & Cooper, D. E. Upconverting Phosphor Reporters in Immunochromatographic Assays. *Anal. Biochem.* **288,** 176–187 (2001).

266. Hong, W., Huang, L., Wang, H., Qu, J., Guo, Z., Xie, C., Zhu, Z., Zhang, Y., Du, Z., Yan, Y., Zheng, Y., Huang, H., Yang, R. & Zhou, L. Development of an up-converting phosphor technology-based 10-channel lateral flow assay for profiling antibodies against Yersinia pestis. *J. Microbiol. Methods* **83,** 133–140 (2010).

267. Li, J. J., Ouellette, A. L., Giovangrandi, L., Cooper, D. E., Ricco, A. J. & Kovacs, G. T. A. Optical Scanner for Immunoassays With Up-Converting Phosphorescent Labels. *Biomed. Eng. IEEE Trans. On* **55,** 1560–1571 (2008).

268. Corstjens, P. L. A. M., de Dood, C. J., Priest, J. W., Tanke, H. J. & Handali, S. Feasibility of a Lateral Flow Test for Neurocysticercosis Using Novel Up-Converting Nanomaterials and a Lightweight Strip Analyzer. *PLoS Negl. Trop. Dis.* **8,** (2014).

269. Mokkapati, V. K., Sam Niedbala, R., Kardos, K., Perez, R. J., Guo, M., Tanke, H. J. & Corstjens, P. L. A. M. Evaluation of UPlink-RSV: Prototype Rapid Antigen Test for Detection of Respiratory Syncytial Virus Infection. *Ann. N. Y. Acad. Sci.* **1098,** 476–485 (2007).

270. Soukka, T., Kuningas, K., Rantanen, T., Haaslahti, V. & Lövgren, T. Photochemical Characterization of Up-Converting Inorganic Lanthanide Phosphors as Potential Labels. *J. Fluoresc.* **15,** 513–528 (2005).

271. Huang, L., Zhou, L., Zhang, Y., Xie, C., Qu, J., Zeng, A., Huang, H., Yang, R. & Wang, X. A Simple Optical Reader for Upconverting Phosphor Particles Captured on Lateral Flow Strip. *IEEE Sens. J.* **9,** 1185–1191 (2009).

272. Ylihärsilä, M., Valta, T., Karp, M., Hattara, L., Harju, E., Hölsä, J., Saviranta, P., Waris, M. & Soukka, T. Oligonucleotide Array-in-Well Platform for Detection and Genotyping Human Adenoviruses by Utilizing Upconverting Phosphor Label Technology. *Anal. Chem.* **83,** 1456–1461 (2011).

273. Hemmilä, I., Dakubu, S., Mukkala, V.-M., Siitari, H. & Lövgren, T. Europium as a label in time-resolved immunofluorometric assays. *Anal. Biochem.* **137,** 335–343 (1984).

274. Kale, V., Soukka, T., Hölsä, J. & Lastusaari, M. Enhancement of blue upconversion luminescence in hexagonal $NaYF_4$:Yb,Tm by using K and Sc ions. *J. Nanoparticle Res.* **15,** 1–12 (2013).

275. Bogdan, N., Vetrone, F., Ozin, G. A. & Capobianco, J. A. Synthesis of Ligand-Free Colloidally Stable Water Dispersible Brightly Luminescent Lanthanide-Doped Upconverting Nanoparticles. *Nano Lett.* **11,** 835–840 (2011).

276. Eaton, D. F. International union of pure and applied chemistry organic chemistry division

commission on photochemistry: Reference materials for fluorescence measurement. *J. Photochem. Photobiol. B* **2,** 523–531 (1988).

277. Xiao, M. & Selvin, P. R. Quantum Yields of Luminescent Lanthanide Chelates and Far-Red Dyes Measured by Resonance Energy Transfer. *J. Am. Chem. Soc.* **123,** 7067–7073 (2001).

278. Kuningas, K., Rantanen, T., Karhunen, U., Lövgren, T. & Soukka, T. Simultaneous Use of Time-Resolved Fluorescence and Anti-Stokes Photoluminescence in a Bioaffinity Assay. *Anal. Chem.* **77,** 2826–2834 (2005).

279. Von Ketteler, A., Herten, D.-P. & Petrich, W. Fluorescence Properties of Carba Nicotinamide Adenine Dinucleotide for Glucose Sensing. *ChemPhysChem* **13,** 1302–1306 (2012).

280. Hönes, J., Wielinger, H. & Unkrig, V. Use of a Sparingly Soluble Salt of a Heteropoly Acid for the Determination of an Analyte, a Corresponding Method of Determination as a Suitable Agent Therefor. US5240860 (A) (1993).